DETECTION OF TELOMERIC DNA CIRCLES IN HUMAN ALT CELLS USING ROLLING CIRCLE AMPLIFICATION

by

Ján Tkáč

B.Sc., The University of Waterloo, 2007

A THESIS SUBMITTED IN PARTIAL FULFILLMENT OF
THE REQUIREMENTS FOR THE DEGREE OF

MASTER OF SCIENCE

in

The Faculty of Graduate Studies
(Medical Genetics)

THE UNIVERSITY OF BRITISH COLUMBIA
(Vancouver)

July 2009

Abstract

Telomeres, the nucleoprotein structures at the ends of linear chromosomes, maintain genomic stability by protecting chromosome ends from fusion, degradation, and processing by the DNA double-strand break repair machinery. Telomere shortening, which occurs naturally in somatic cells during aging, leads to cellular senescence or apoptosis. In contrast, germline cells and cancer cells acquire unlimited replicative potential by activating a telomere lengthening mechanism, generally via reactivating the enzyme telomerase reverse transcriptase. To date, drug development targeting cellular immortalization in cancer has focused on telomerase inhibition. However, in a subset of tumours and *in vitro*-immortalized cell lines, telomeres are maintained by homologous recombination-mediated pathways, termed alternative lengthening of telomeres (ALT). ALT tumours are expected to be refractory to anti-telomerase therapies, so the ability to rapidly and reliably screen for ALT status in tumour-derived cells is essential for guiding therapeutic strategies that target cellular immortalization. One characteristic of ALT-mediated telomere maintenance is the presence of extrachromosomal telomeric repeat-containing DNA circles (t-circles), which provide an attractive target for detection in screening applications. Current methods of t-circle detection require considerable amounts of cells, making them unsuitable for analysis of limited clinical samples. We optimized a screen for ALT status based on a novel technique of rolling circle amplification (RCA) of t-circles from extrachromosomal DNA extracts of human ALT cells. We demonstrate that RCA requires a much lower number of cells than previously established t-circle detection methods, and screening many samples can be performed in parallel, making RCA suitable for analyzing clinical samples. T-circles were reproducibly detected in human immortalized ALT cell lines, but not in telomerase-utilizing cell lines. In addition, ectopic over-expression of telomerase in an ALT cell line does not appear to affect t-circle formation. This suggests that presence of active telomerase within a cell does not inhibit all telomeric recombination reactions. The potential for RCA as a tool to screen tumour samples for ALT activity and the link between telomerase and ALT-based telomere lengthening mechanisms are discussed.

Table of Contents

List of Tables

List of Figures

List of Abbreviations

ALT	Alternative lengthening of telomeres
APB	Alternative lengthening of telomeres-associated promyelocytic leukemia nuclear body
CO-FISH	Chromosome orientation fluorescence *in situ* hybridization
D-loop	Displacement loop
dsDNA	Double-stranded DNA
ecDNA	Extrachromosomal DNA
EM	Electron microscopy
EtBr	Ethidium bromide
FACS	Fluorescence-activated cell sorting
GFP	Green fluorescent protein
HJ	Holliday junction
IRES	Internal ribosome entry site
LTR	Long terminal repeat
MSCV	Murine stem cell virus
mtDNA	Mitochondrial DNA
PD	Population doubling
2D PFGE	Two-dimensional pulsed-field gel electrophoresis
PGK	Phosphoglycerin kinase
PML	Promyelocytic leukemia protein
POT1	Protection of telomeres 1
Q-FISH	Quantitative fluorescence *in situ* hybridization
Rad50/51/52	Radiation sensitive isolate 50/51/52
Rap1	Repressor/activator protein 1
RCA	Rolling circle amplification
SCE	Sister chromatid exchange
SSB	Single-stranded DNA binding protein
ssDNA	Single-stranded DNA
SV40	Simian virus 40
T-circle	Telomeric repeat-containing circular DNA molecule
T-loop	Telomere loop
T-SCE	Telomeric sister chromatid exchange
TERT	Telomerase reverse transcriptase catalytic subunit
TIN2	TRF1-interacting nuclear factor 2
TPP1	TIN2- and POT1-interacting protein 1
TR	Telomerase RNA component
TRAP	Telomere repeat amplification protocol
TRF	Terminal restriction fragment
TRF1/2	Telomeric repeat binding factor 1/2
YFP	Yellow fluorescent protein

Acknowledgements

I would like to thank Dr. Peter Lansdorp for giving me the opportunity to be part of this truly exciting field of research and for all his advice.

All members of the Lansdorp laboratory for providing scientific discussion, technical advice, and most importantly, a terrific work environment.

Dr. Karel Riha (Gregor Mendel Institute, Vienna, Austria) for sharing his rolling circle amplification protocol.

Dr. David Huntsman, Dr. Louis Lefebvre, and Dr. Ann Rose, for their insight and helpful discussion of this study.

Dr. Ester Falconer and Dr. Mark Hills for critically reviewing this dissertation.

This work was largely funded by a Natural Sciences and Engineering Research Council of Canada (NSERC) Postgraduate Scholarship.

Dedication

Túto prácu venujem mojim rodičom, Ivanovi Tkáčovi a Ružene Tkáčovej.
Ďakujem Vám za pomoc a hlavne za lásku, ktorou ma neustále obohacujete.
Ďakujem Vám, že som, kto som.

Chapter 1: Introduction

1.1 Telomeres

Seminal experiments, performed more than 60 years ago by Hermann Müller and Barbara McClintock, provided initial glimpses into the biological importance of the structures that cap the ends of linear chromosomes. Müller, studying chromosomal rearrangements in *Drosophila melanogaster*, observed that deletions and inversions of chromosome ends are extremely rare [Müller, 1938]. He posited that chromosome stability requires specialized terminal structures, which he called "telomeres" [Zakian, 1989]. McClintock, studying chromosome dynamics in *Zea mays*, noted that broken chromosomes have a tendency to fuse with one another, whereas natural chromosome ends are stable and do not fuse with broken ends or with one another [McClintock, 1941]. These and numerous subsequent studies established that telomeres have important functions in protecting chromosome ends from fusion and degradation, thus stabilizing chromosomes to ensure faithful DNA replication of the entire "coding" genome and proper segregation of genetic material into daughter cells upon cell division. These functions are indispensable for cellular fidelity and survival in all organisms with linear genomes. In the following sections, the current understanding of telomere structure and function is summarized along with the molecular mechanisms used to maintain functional telomeres.

1.1.1 Telomere structure

Telomeres are nucleoprotein complexes that cap the ends of linear chromosomes. The DNA sequence of vertebrate telomeres consists of tandem arrays of 5′-$(TTAGGG)_n$-3′ repeats [de Lange *et al.*, 1990; Moyzis *et al.*, 1988]. The majority of the telomeric tract is double-stranded (dsDNA); however, telomeres terminate in a single-stranded (ssDNA) overhang of the 3′-G-rich strand, which is 130-210 nucleotides in length [Allshire *et al.*, 1989; de Lange *et al.*, 1990; Makarov *et al.*, 1997]. This 3′-G-rich overhang is crucially important for telomere capping function and for protection of chromosomal integrity [Henderson *et al.*, 1987; Henderson and Blackburn, 1989]. The capping mechanism in mammalian cells relies on the folding of telomeric DNA and strand invasion of the 3′-G-rich overhang into proximal duplex telomeric tracts, resulting in the formation of a lariat structure called the telomere loop, or t-loop [Griffith *et al.*, 1999]. The t-loop sequesters the free end of the chromosome, preventing inappropriate DNA repair reactions and activation of DNA damage checkpoints. A simplified schematic of t-loop formation and stabilization by protein binding is shown in Figure 1.1.

T-loops are stabilized by several telomere-binding proteins. Six proteins – telomeric repeat binding factor (TRF) 1, TRF2, protection of telomeres 1 (POT1), TRF1-interacting nuclear factor 2 (TIN2), repressor/activator protein 1 (Rap1), and TIN2- and POT1-interacting protein 1 (TPP1) – are constitutively localized to telomeres, although their exchange at telomeric sites is very dynamic [Mattern *et al.*, 2004]. Together, these proteins form a complex known as "shelterin" [de Lange, 2005]. TRF1 and TRF2 interact with telomeric dsDNA, whereas POT1 binds the ssDNA G-rich overhang (Figure 1.1A. Rap1, TPP1, and

TIN2 interact directly with the TRF1/TRF2 protein complexes [Aubert and Lansdorp, 2008]. TRF1 and TRF2 can fold telomeric DNA, stimulating t-loop formation (Figure 1.1B) [Amiard *et al.*, 2007; Bianchi *et al.*, 1997]. In addition, TRF2 stabilizes t-loops by promoting the formation and protecting from cleavage the Holliday junction (HJ)-like structure that occurs at the site of strand invasion of the 3′-G-rich overhang into proximal duplex telomeric sequences (Figure 1.1C) [Poulet *et al.*, 2009]. Strand invasion produces an internal ssDNA displacement loop (D-loop), which is stabilized by binding of POT1 [de Lange, 2005].

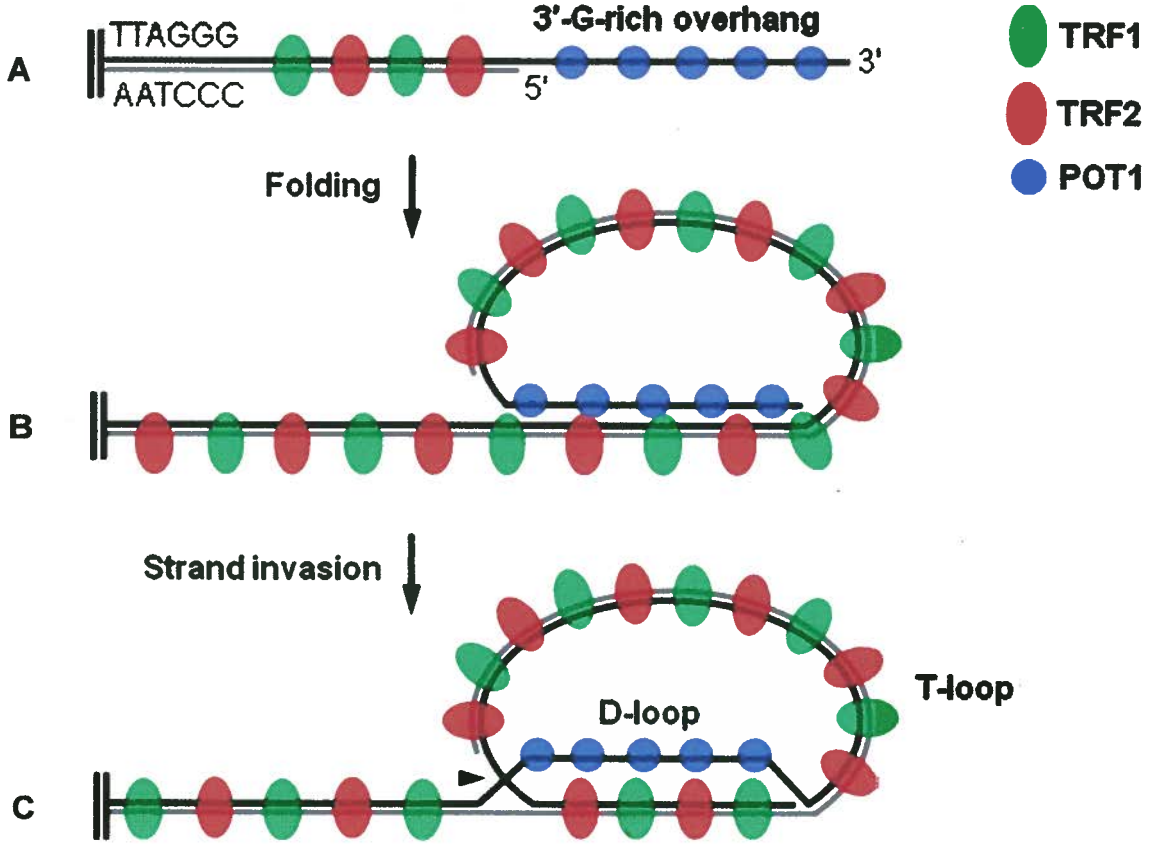

Figure 1.1 Telomeres form a protective cap sequestering the 3′-G-rich overhang into a t-loop. (A) "Open" telomere conformation with an exposed ssDNA 3′-G-rich overhang. (B) TRF1 and TRF2 bend telomeric DNA upon binding. (C) "Closed" telomere conformation results from TRF2-stimulated strand invasion of the 3′-G-rich overhang into proximal telomeric regions, forming the t-loop. A ssDNA D-loop created at the site of strand invasion is stabilized by binding of POT1. The arrowhead indicates the HJ-like structure formed at the site of strand invasion.

1.1.2 Telomere function and maintenance

To form t-loops and protect chromosomes from degradation or fusion, telomeres must have a certain length. Telomere attrition results from several cellular processes and accompanies organismal aging in long-lived species [Aubert and Lansdorp, 2008]. Small consistent losses occur due to the "end-replication problem", whereby gradual shortening is observed after each replication of linear DNA molecules [Olovnikov, 1973]. The end-replication problem results from the inability of conventional DNA polymerases to replicate the 5′ end of linear chromosomes during lagging strand synthesis [Watson, 1972]. For human somatic cells *in vitro*, the end replication problem and post-replication exonucleolytic processing of the 5′-C-rich strand result in a telomere length decline of 50-150 base pairs (bp) with each population doubling [Martens *et al.*, 2000]. In addition, larger sporadic truncations may occur via stochastic events, such as failure to repair oxidative damage to telomeric DNA, failure to properly process higher-order structures of G-rich DNA, and homologous recombination reactions [Lansdorp, 2005]. Loss of telomeric DNA eventually leads to growth arrest accompanied by cellular senescence and apoptosis [Martens *et al.*, 2000]. Senescence is induced when shorter telomeres, which are likely unable to form stable t-loops and thus perform their protective functions, are recognized by the DNA repair machinery as DNA double-strand breaks [d'Adda di Fagagna *et al.*, 2003]. Since cancer cells require many cell divisions to form tumours, by limiting the cellular replicative capacity, telomere attrition serves as a tumour suppressor mechanism in long-lived multicellular organisms, including humans [Aubert and Lansdorp, 2008].

Germline cells and some somatic cells, such as B lymphocytes, must maintain their replicative capacity and therefore maintain telomere length throughout the life of the organism. In these cells, telomeres are continuously maintained by the enzyme telomerase, the ribonucleoprotein reverse transcriptase capable of *de novo* addition of telomeric repeats to the 3' end of the telomere. First discovered in the ciliate protozoan *Tetrahymena* [Greider and Blackburn, 1985; Greider and Blackburn, 1987], telomerase has since been identified in eukaryotes as diverse as fungi, plants, and mammals, including humans [Aubert and Lansdorp, 2008]. The minimal telomerase enzyme consists of the telomerase reverse transcriptase (TERT) catalytic subunit, and the telomerase RNA component (TR), which folds into a secondary structure with an exposed telomere repeat template region. TERT catalyzes the addition of telomeric repeats to the 3'-G-rich strand using the TR RNA subunit as template.

While telomerase activity is detectable in the germline and in some stem cells, most somatic cells have little or no detectable telomerase activity. Thus, cells of the soma undergo telomere shortening until the telomeres are too short to form a protective cap and become recognized as double-strand breaks by the DNA repair machinery, inducing a signaling cascade leading to cellular senescence [d'Adda di Fagagna *et al.*, 2003]. However, some cells may continue to divide post-senescence with increasing genomic instability due to uncapped telomeres. These cells eventually reach a point called crisis, where the majority of cells die by apoptosis. Sporadically, a minority of cells in crisis acquires the ability to lengthen telomeres, becoming immortalized (gaining unlimited replicative potential). Somatic cellular immortalization *in vivo* leads to tumorigenic growth. In humans, immortalization occurs via

two general mechanisms. The majority of cancer cells express and utilize telomerase for immortalization; however, about 10 % of cancers and up to 40 % of *in vitro*-immortalized cell lines utilize a poorly-understood, recombination-mediated pathway termed alternative lengthening of telomeres (ALT) [Bryan *et al.*, 1995; Muntoni and Reddel, 2005; Murnane *et al.*, 1994]. An illustration of telomere length dynamics with increasing cell divisions is shown in Figure 1.2.

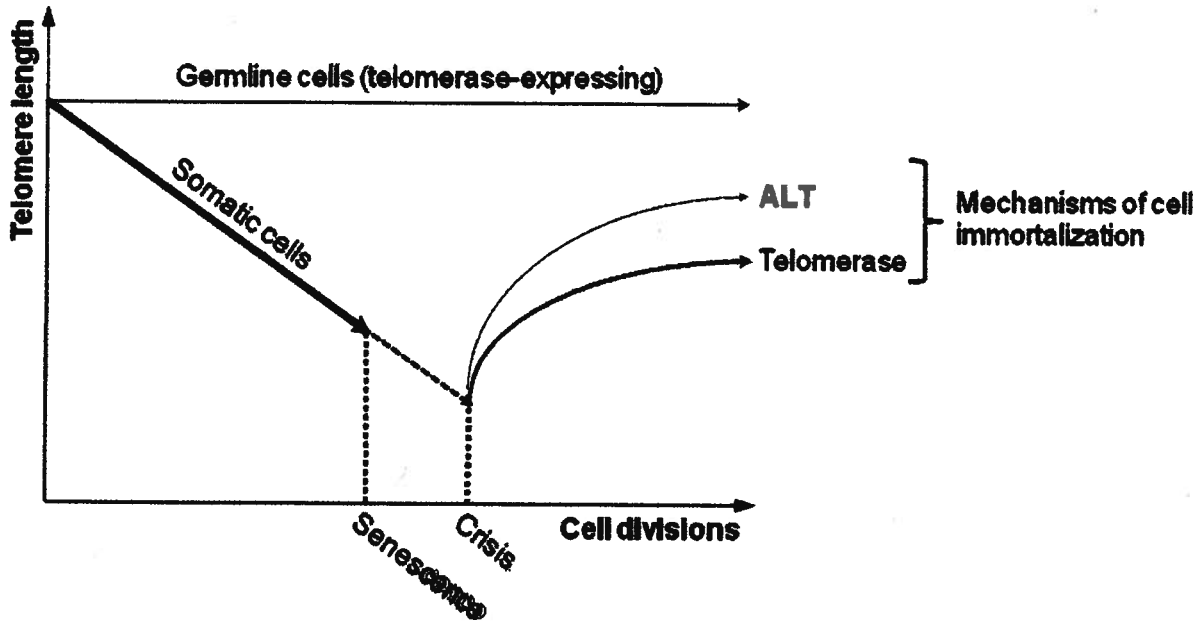

Figure 1.2 Telomere length is under strict regulatory control. Telomere length is constitutively maintained in cells of the germline by telomerase. In somatic cells, which do not express telomerase, telomere length declines at a predictable rate with increasing cell divisions, as well as via unpredictable stochastic telomere truncation events. When telomeres become too short to perform their chromosome protective functions, senescence ensues. Some cells continue to divide pots-senescence until reaching a point of unbearable genomic instability in crisis, where most cells undergo apoptosis. Sporadic survivors emerge out of crisis by activating a telomere maintenance mechanism, either telomerase or ALT (indicated in red). These immortalized cells can lead to cancer.

1.2 Alternative lengthening of telomeres (ALT)

ALT is defined by the ability of a cell to maintain its telomeres and replicate indefinitely in the absence of detectable telomerase activity [Kim *et al.*, 1994]. Human ALT cell lines have undetectable expression of the full length hTERT transcript [Kilian *et al.*, 1997]. The definition of ALT is somewhat problematic, as it is based on the absence of a particular phenotypic marker (telomerase activity) and not on the presence of any specific phenotype. Thus, many studies since the first identification of human ALT cells [Bryan *et al.*, 1995; Murnane *et al.*, 1994], have focused on characterizing the ALT phenotype beyond its non-reliance on telomerase. This work has resulted in the identification of some common phenotypic features identified in subsets of ALT cells. These include telomeric recombination and sister chromatid exchange (SCE) events, a distinct telomere length profile, presence of ALT-associated promyelocytic leukemia (PML) nuclear bodies (APBs), instability at a specific DNA minisatellite (MS32), and presence of telomeric repeat-containing extrachromosomal DNA (ecDNA) [Royle *et al.*, 2008]. These characteristics have been observed in some, but not all human ALT cells. Due to this phenotypic heterogeneity associated with ALT, it is likely that multiple molecular pathways of telomere lengthening in a non-telomerase setting are in existence [Stewart, 2005]. However, the overriding theme of the commonalities between different ALT cells is that ALT constitutes recombination-mediated telomere maintenance, potentially involving inter- and intramolecular homologous recombination reactions, gene conversion-like events, and templating of telomere extension by telomeric ecDNA molecules [Henson *et al.*, 2002].

1.2.1 ALT is a recombination-mediated mechanism

Recombination-mediated telomere elongation has been most studied in yeast, where it occurs in mutants that lack telomerase [Lendvay *et al.*, 1996; Lundblad and Szostak, 1989; Lundblad and Blackburn, 1993; McEachern and Blackburn, 1996; Teng and Zakian, 1999]. In *Saccharomyces cerevisiae*, deletion of telomerase leads to gradual telomere shortening over 50-100 generations, eventually resulting in growth senescence [Lundblad and Blackburn, 1993]. Only a minority of cells is able to bypass this replicative block and can continue to be serially streaked. These survivors rely on homologous recombination mechanisms to maintain telomeres, as evidenced by their dependence on Radiation sensitive isolate 52 (Rad52), a recombinase protein that is required for a majority of mitotic recombination reactions [Lundblad and Blackburn, 1993; Teng and Zakian, 1999]. The unusual arrangement of chromosome ends in *S. cerevisiae*, with telomeric repeat arrays separated by 6-7 kb subtelomeric elements termed Y′, leads to the emergence of two main types of survivors. These employ distinct pathways of telomeric recombination. Type I survivors are Rad51-dependent, and are typified by amplification of the subtelomeric Y′ elements and very short tracts of telomeric repeats. Type II survivors are Rad50-dependent and lack the Y′ amplification, but instead display greatly amplified telomeric repeat DNA [Lundblad and Blackburn, 1993]. It has been proposed that *S. cerevisiae* type II recombination is mechanistically similar to the mammalian ALT pathway [Lustig, 2003].

Unambiguous evidence that the ALT mechanism in human cells relies on some form of telomere-telomere recombination was provided by experiments wherein a plasmid DNA tag that had been targeted to some telomeres within an ALT cell clone had been propagated to a

number of other telomeres over the course of several population doublings (PDs) [Dunham *et al.*, 2000]. There was a progressive increase in the number of tagged telomeres with increasing PDs. This phenomenon was not seen when the tag was inserted into the subtelomeric region in ALT cells, nor when inserted into the telomeres of telomerase-utilizing cell lines. This suggests that increased recombination rates are restricted to the telomeres in ALT cells and that telomeric recombination does not occur in telomerase-utilizing cells. In subsequent years, evidence for inter- and intra-telomeric recombination and gene conversion-like events at the telomeres in ALT cells has been accumulated [Muntoni *et al.*, 2009; Varley *et al.*, 2002].

In addition, telomeric sister chromatid exchange (T-SCE) events (recombination between sister chromatids on the same chromosome), which are extremely rare in mortal and telomerase-immortalized cells, occur with a high frequency in ALT cells [Londoño-Vallejo *et al.*, 2004]. Similarly to inter-chromosomal telomeric recombination events described above, the increased frequency of SCEs is limited to the telomeres in ALT cells, because no correlation was found with SCE rates at non-telomeric chromosome sites, and T-SCEs were not observed in non-ALT, Bloom syndrome cells which have very high global SCE rates [Londoño-Vallejo *et al.*, 2004].

1.2.2 Telomere length in ALT cells

ALT cells have a telomere length phenotype that is distinct from telomerase-expressing immortal cells. The telomere length in human telomerase-utilizing cell lines is relatively short and homogeneous, with a mean telomere length of less than 10 kb [Bryan *et al.*, 1995;

Park *et al.*, 1998]. In contrast, human ALT cells have a very heterogeneous distribution of telomere lengths, ranging from a few hundred base pairs to over 50 kb, with a mean length of approximately 20 kb [Bryan *et al.*, 1995; Jeyapalan *et al.*, 2008]. Furthermore, telomere lengths are heterogeneous within individual ALT cells, as evidenced by telomere visualization using quantitative fluorescence *in situ* hybridization (Q-FISH) of telomere repeat probes on metaphase chromosomes in mouse and humans [Hande *et al.*, 1999; Perrem *et al.*, 2001]. Some chromosome ends have no detectable telomere sequence, whereas others within the same cell have very strong telomere signal. In cells that become immortalized in the absence of telomerase activity during *in vitro* culturing, the timing of the immortalization event (overgrowth of a culture in crisis by immortalized cells) correlates with rapid telomere lengthening and generation of length heterogeneity that are characteristic of the ALT mechanism [Yeager *et al.*, 1999].

1.2.3 ALT-associated promyelocytic leukemia nuclear bodies

The majority of ALT cell lines analyzed to date contain subnuclear structures called ALT-associated promyelocytic leukemia (PML) nuclear bodies (APBs) [Yeager *et al.*, 1999]. PML nuclear bodies are punctate proteinaceous structures bound to the nuclear matrix in the cells of most, but not all tissues [Henson *et al.*, 2002; Stuurman *et al.*, 1992]. Numerous proteins transiently localize to the PML bodies, which seem to be extremely functionally diverse [Bernardi and Pandolfi, 2007]. PML nuclear bodies have been implicated in numerous cellular processes. These include tumour suppression, cell cycle regulation, senescence, apoptosis, inflammatory responses, antigen presentation, protein refolding and degradation, and differentiation [Henson *et al.*, 2002].

In ALT cells, about 5 % of nuclei contain PML bodies that co-localize with telomeric DNA and/or telomere-associated proteins such as TRF1 and TRF2 [Yeager *et al.*, 1999]. These ALT-specific structures are termed APBs. APB function is not well understood, but it has been suggested that they may serve as repositories for proteins required for the ALT pathway [Royle *et al.*, 2008]. In various studies, APBs were shown to contain numerous proteins known to function in DNA replication, recombination, and repair: RAD51, RAD52, RPA, MRE11, RAD50, NBS1, BLM and WRN [Johnson *et al.*, 2001; Wu *et al.*, 2000; Wu *et al.*, 2003; Yankiwski *et al.*, 2000; Yeager *et al.*, 1999]. Cell cycle analysis has shown that large APBs are most abundant during the G2 phase of the cell cycle, which coincides with the timing of telomere elongation in ALT cells [Grobelny *et al.*, 2000] This data suggests that APBs may be the site for telomere elongation in ALT cells, however there is no direct evidence for this. Telomeric-repeat containing ecDNA molecules (discussed in detail in Section 1.2.5) also localize to APBs [Muntoni and Reddel, 2005]. Interestingly, short linear extrachromsomal fragments preferentially localize within APBs and it was proposed that such localization may allow the cell to evade the DNA damage response triggered by the unprotected DNA ends [Fasching *et al.*, 2007].

1.2.4 Instability at minisatellite MS32

Although T-SCEs are elevated in ALT cells, the frequency of SCE at non-telomeric sites is not increased relative to telomerase-utilizing immortal cells [Londoño-Vallejo *et al.*, 2004]. Likewise, the overall frequency of homologous recombination is similar in ALT and telomerase-utilizing cell lines [Bechter *et al.*, 2003]. Thus the recombination-mediated telomere maintenance in ALT cells does not appear to be accompanied by a global increase

in recombination frequency. In light of this information, it was surprising that a specific minisatellite (a tandem array of 10 – 100 bp repeats [Sudbery, 2002]), MS32 was found to be highly unstable in a subset of ALT cell lines, but not in telomerase-utilizing or mortal cells [Jeyapalan *et al.*, 2005]. MS32 instability was also found in a subset of ALT-utilizing sarcomas, indicating that MS32 instability occurs *in vivo* and is not simply a cell culture artifact. The MS32 minisatellite is located on the distal portion of chromosome 1 (1q42.3) and consists of a tandem array of 29 bp repeats [Royle *et al.*, 2008]. It is relatively GC-rich (~65 %), which may be indicative of a common mutational mechanism with telomeric DNA. Six other minisatellites (MS31A, CEB1, MS205, B6.7, MS1, DXYS14) distributed on various chromosomes did not show increased instability in ALT cells [Jeyapalan *et al.*, 2005; Royle *et al.*, 2008]. The initiation of MS32 instability coincides with activation of ALT, suggesting an overlap between the underlying mechanisms and possibly between the proteins involved [Royle *et al.*, 2008]. Apart from these associations, it is currently unclear why this specific minisatellite is so highly mutable in ALT cells.

1.2.5 Telomeric circles (t-circles) and other telomeric extrachromosomal DNA (ecDNA) molecules

ALT cells contain a significant amount of telomeric repeat-containing ecDNA which can be linear or circular [Cesare and Griffith, 2004; Ogino *et al.*, 1998; Tokutake *et al.*, 1998; Wang *et al.*, 2004; Yeager *et al.*, 1999]. These molecules are thought to arise by homologous recombination events between telomeric repeats. Recently, a detailed study of the structures of telomeric DNA molecules in ALT cells showed that the majority of telomeric ecDNA consists of dsDNA circles and ssDNA of the G-rich strand [Nabetani and Ishikawa, 2009].

The study further identified a novel form of telomeric ecDNA, termed "t-complex" DNA, which consists of highly branched molecules thought to represent complex homologous recombination intermediates. Circular telomeric ecDNA molecules (known as telomeric circles or t-circles) are particularly interesting in the context of ALT, because they could be produced by intramolecular recombination within the characteristic long telomeres and may potentially serve as templates for telomere elongation by a rolling circle amplification mechanism [Natarajan and McEachern, 2002]. T-circles are characteristic of the yeast type II survivor recombination mechanism (see Section 1.2.1), which results in amplification of telomeric DNA [Nosek *et al.*, 2006]. Furthermore, t-circles have been observed in a variety of distantly-related organisms, including yeast, plants, amphibians, and mammals (reviewed by [Tomaska *et al.*, 2004]).

1.3 Proposed mechanisms of t-circle generation in ALT cells

T-circles have been identified in a number of cell lines which maintain telomeres by the ALT mechanism [Cesare and Griffith, 2004; Wang *et al.*, 2004]. The generation of t-circles in ALT cells relies on homologous intramolecular recombination between telomeric repeats [Dunham *et al.*, 2000; Henson *et al.*, 2002]. Although the exact mechanism of this process has not been elucidated, several models have been proposed (Figure 1.3). Currently, the most popular model of t-circle formation is based on a process termed "t-loop excision", which results from recombination-mediated resolution of the Holliday junction-like structure (Figure 1.1C) formed at the site of strand invasion of duplex telomeric DNA by the single-stranded 3′ G-rich overhang (Figure 1.3A). This process has been described in yeast type II survivors and also in Rap1 mutants, which undergo telomere rapid deletion events [Lustig,

2003]. In human cell lines, evidence of t-loop excision came from studies where expression of a mutant allele of TRF2 ($TRF2^{\Delta B}$) in several cell types caused massive sudden telomere loss [Wang *et al.*, 2004]. This telomere shortening was accompanied by the generation of t-loop-sized t-circles in $TRF2^{\Delta B}$-expressing cells. In this study, t-circle formation was dependent on XRCC3, a Rad51-related protein associated with Holliday junction resolvase activity *in vitro* [Liu *et al.*, 2004]. In addition to t-loop excision, t-circles may also arise by intramolecular recombination between duplex telomeric DNA tracts (Figure 1.3B) or by ligation of linear telomeric ecDNA fragments (Figure 1.3C) [Tomaska *et al.*, 2004].

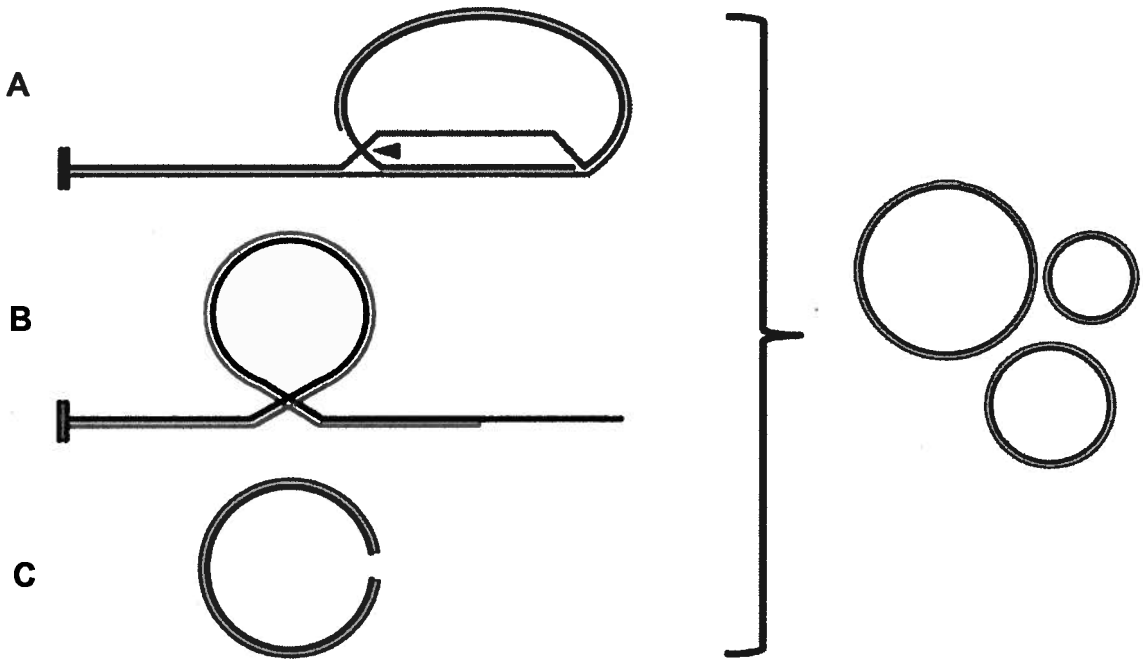

Figure 1.3 Potential mechanisms of t-circle formation in ALT cells. (A) T-loop excision. (B) Intramolecular homologous recombination. (C) Circularization of linear telomeric ecDNA. [Tomaska *et al.*, 2004]

1.4 Proposed mechanisms of telomere elongation mediated by t-circles

Several mechanisms have likewise been proposed for telomere lengthening mediated by t-circles. T-circles may serve as templates for telomere extension by a rolling circle amplification (RCA) mechanism, primed by the 3′-G-rich overhang. The overhang could invade duplex t-circles or bind to C-rich ssDNA t-circles (Figure 1.4A). Branch migration of the overhang would allow essentially unlimited elongation of the chromosomal telomere [Henson *et al.*, 2002]. Linear telomeric ecDNA fragments could likewise be extended by RCA on a t-circle template (Figure 1.4B). Subsequent recombination with telomeres or copying of the elongated linear ecDNA by a gene conversion-like mechanism could lengthen chromosomal telomeres. Intermolecular recombination mechanisms may also mediate direct integration of t-circles into duplex telomeric DNA (Figure 1.4C).

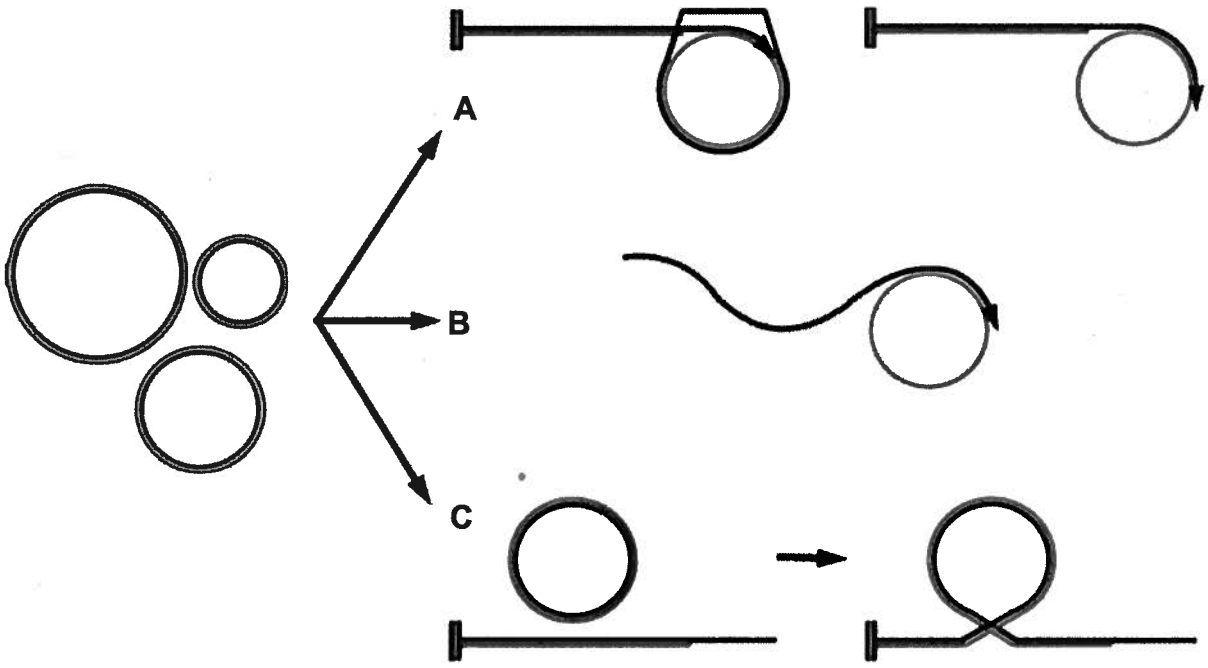

Figure 1.4 Potential mechanisms of telomere elongation mediated by t-circles. (A) Rolling circle amplification using dsDNA or ssDNA t-circles as templates. (B) Rolling circle amplification of linear telomeric ecDNA. (C) Recombinational integration of a t-circle. [Tomaska *et al.*, 2004]

1.5 ALT in cancer

The vast majority of human cancers actively maintain telomere lengths, allowing the tumour cells unlimited replicative potential. Surveys across many types of cancer have revealed that approximately 90 % express telomerase and thereby maintain a stable and homogeneous telomere length [Kim *et al.*, 1994]. The remaining 10 % of tumours activate the ALT pathway of telomere maintenance [Bryan *et al.*, 1995]. However, the prevalence of ALT activation in specific cancer types, such as some tumours of mesenchymal origin appears to be much higher. For example, about 47 % of osteosarcomas, 25 % of liposarcomas, and 34 % of astrocytomas activate ALT [Costa *et al.*, 2006; Henson *et al.*, 2005; Johnson *et al.*, 2005]. The reasons for this tissue specificity in the utilization of ALT are not yet understood, but it has been proposed that expression of the telomerase reverse transcriptase catalytic subunit (TERT) may be more heavily repressed in tissues of mesenchymal origin [Henson *et al.*, 2002].

To date, therapies targeting cellular immortalization in cancer have focused on inhibition of telomerase. However, as discussed above, a significant number of cancers utilize ALT for telomere maintenance and resultant acquisition of limitless replicative capacity. These tumours are expected to be refractory to telomerase-targeting therapies. Indeed, it has been shown that introduction of a dominant-negative form of hTERT into the GM847 human ALT cell line did not affect telomere length nor cell growth; whereas introduction of the same dominant-negative hTERT mutant in telomerase-utilizing tumour cell lines caused telomere shortening and induced cell death [Hahn *et al.*, 1999]. It has been further suggested that ALT may constitute an escape mechanism for telomerase-utilizing tumours treated with anti-

telomerase therapies, by selecting for ALT cells within a given tumour mass [Henson *et al.*, 2002; Stewart, 2005]. Similarly, primary telomerase-utilizing tumours may give rise to ALT-utilizing secondary tumours, as evidenced by observation of a patient with a telomerase-positive glioblastoma multiforme who presented with an ALT-positive recurrent tumour [Hakin-Smith *et al.*, 2003].

1.6 Objectives and rationale

To guide treatment strategies that target cellular immortalization, it is essential to develop a robust method for determining ALT status in tumours and tumour-derived cell lines.

Whether t-circles are a by-product or active mediators of telomeric recombination processes, their presence in ALT cells makes them an attractive target for detection in screening applications. Currently, the most commonly used method of t-circle detection is neutral-neutral 2-dimensional pulsed-field gel electrophoresis (2D PFGE). 2D PFGE is based on the electrophoretic separation of DNA molecules by size (i.e., molecular weight) in the first dimension and by molecular structure/topology (e.g., linear vs. circular, "relaxed" vs. supercoiled) in the second dimension. T-circles migrate through the gel in the second dimension (separation by molecular structure or shape) at a slower rate relative to linear telomeric DNA [Wang *et al.*, 2004]. This method requires that digested genomic DNA from approximately 1.5-3.5 x 10^6 human diploid cells is loaded in a single 2D gel [Cesare and Griffith, 2004; Wang *et al.*, 2004; Wang *et al.*, 2004]. The requirement for these large samples precludes analysis of clinical tumour-derived cells, if these are low in number. An additional drawback of 2D PFGE is that only a single sample can be loaded in a 2D gel, so

evaluation of numerous samples requires several gels and additional controls for between-gel variability of hybridization efficiency and exposure differences between different X-ray films.

These problems may be overcome using a novel, rolling circle amplification (RCA)-based method of t-circle detection. (A detailed comparison of RCA and 2D PFGE t-circle detection methods is provided in Chapter 4: Discussion.) An RCA-based t-circle assay detected t-circles in DNA extracts from *Arabidopsis thaliana* mutant cells which maintain telomeres by homologous recombination [Zellinger *et al.*, 2007]. Using telomeric sequence-specific primers and a highly-processive DNA polymerase from phage Φ29, t-circles were amplified by RCA and detected by denaturing agarose gel electrophoresis and subsequent probing.

Our primary goal was to adapt this RCA-based method for the detection of t-circles in human immortalized cell lines. Using RCA, t-circles may potentially be detected with much higher sensitivity and many samples may be analyzed in parallel on a single denaturing gel. These potential advantages of RCA over currently-used t-circle detection methods may allow for development of a reliable screen for ALT status with potential clinical applicability.

Our secondary goal was to examine the effects of telomerase on telomere maintenance by the ALT pathway, by determining whether reconstitution of telomerase activity in ALT cells affects t-circle generation.

Chapter 2: Materials and methods

2.1 Cell culture

Cell lines HeLa, GM847, and SUSM-1, were grown in Dulbecco's Modified Eagle Medium with 4.5 g/L D-glucose (STEMCELL Technologies, Vancouver, Canada), supplemented with 10 % fetal calf serum (FCS), 2 mM L-glutamine, 100 U/mL penicillin, and 100 µg/mL streptomycin. WI-38 VA-13 subline 2RA (VA-13) fibroblasts and PG-13 virus packaging cells were grown in Modified Eagle Medium-α (Invitrogen, Carlsbad, CA, U.S.A.) supplemented with 10 % FCS, 2 mM L-glutamine, 100 µM MEM non-essential amino acid solution, 100 U/mL penicillin, and 100 µg/mL streptomycin. HCT116 cells were grown in McCoy's 5A Medium (Invitrogen, Carlsbad, CA, U.S.A.) supplemented with 10 % FCS, 2 mM L-glutamine, 100 U/mL penicillin, and 100 µg/mL streptomycin. All cells were incubated at 37 °C and 5 % CO_2 for expansion.

2.2 Extrachromosomal DNA isolation

ecDNA was isolated using a modified Hirt extraction procedure [Hirt, 1967]. 2 x 10^6 cells were washed twice in phosphate-buffered saline (PBS), resuspended in 400 µL of lysis buffer (10 mM Tris-HCl, pH 7.5; 10 mM EDTA, pH 8.0; 0.6 % SDS) and incubated for 5 minutes at room temperature. 100 µL of 5 M NaCl was added to each tube and mixed thoroughly by inverting the tube 4-5 times. The samples were incubated overnight at 4 °C, followed by centrifugation at 13,000 r.p.m. for 30 min at 4 °C, in a tabletop centrifuge. The chromosomal DNA pellet was discarded and the ecDNA was extracted from the supernatant using phenol:chloroform:isoamyl alcohol (25:24:1, w/v). ecDNA was precipitated using 1 mL (2

volumes) of absolute isopropanol and 50 µL (0.1 volumes) of 3M sodium acetate (pH5.2), then washed in 500 µL 70 % ethanol and air dried. ecDNA was resuspended in 65 µL of Tris-EDTA buffer (TE) containing 20 µg/mL RNase A and incubated at 37 °C for 30 min to digest any RNA in the sample. The isolated ecDNA samples were quantified using a NanoDrop spectrophotometer (Thermo Fisher Scientific, Waltham, MA, U.S.A.) stored at -20 °C until use.

2.3 Rolling circle amplification

The oligonucleotide used to prime the RCA reaction was telomeric sequence 21mer ("thio-C": 5′-CCCTAACCCTAACCCTAACsCsC-3′), containing two thiophosphate linkages (denoted by "s") between the three 3′ terminal nucleotides (University of Calgary Core DNA Services, DNA/RNA Synthesis Laboratory, Calgary, Canada).

In a 0.2 mL PCR tube, we combined 6.5 µL of ecDNA extract (2 x 10^5 cell-equivalents), 2.5 µL of 1 µM thio-C primer, and 1 µL of 10 x annealing buffer (200 mM Tris-HCl, pH 7.5; 1 mM EDTA, pH 8.0; 0.2 M KCl). The mixture was covered with a drop of mineral oil, denatured at 95 °C for 3 min, and then placed on ice for 15 min to anneal the thio-C primer to complementary telomeric sequences in the ecDNA extract. The total RCA reaction volume was 20 µL, containing the post-annealing DNA mixture, 0.2 mM dNTP mix, 33 mM Tris-acetate (pH 7.9), 10 mM magnesium acetate, 66 mM potassium acetate, 0.1 % (v/v) Tween 20, 1 mM DTT, 50 µg/mL *Escherichia coli* single-stranded DNA binding protein (USB, Cleveland, OH, U.S.A.), and 7.5 U of Φ29 DNA polymerase (Fermentas, Burlington, Canada). RCA was carried out at 30 °C for 16 hr. Φ29 DNA polymerase was inactivated by

incubation at 65 °C for 10 min. Only extracts from cell lines which contain t-circles provide appropriate templates for amplification by RCA under these conditions.

2.4 In-gel detection of RCA reaction products

Half of the RCA reaction product (10 μL) was loaded onto a denaturing agarose gel (0.8 % agarose; 50 mM NaOH; 1 mM EDTA, pH 8.0) and separated by electrophoresis in alkaline running buffer (50 mM NaOH; 1 mM EDTA, pH 8.0) at approximately 2 V/cm for 16-18 hr. The gel was stained with SYBR Green II (Invitrogen, Carlsbad, CA, U.S.A.), which preferentially binds RNA and ssDNA for 40 min at room temperature and imaged using Quantity One gel analysis software (Bio-Rad Laboratories, Hercules, CA, U.S.A.). The gel was baked at 60 °C for 45 min under vacuum. The flattened gel was denatured (0.5 M NaOH, 1.5 M NaCl) for 20 min and neutralized (0.5 M Tris-HCl, pH 7.5; 1.5 M NaCl) for 20 min.

The gel was pre-hybridized in 6X SSC, 0.1 % SDS for 1 hr at 37 °C. The gel was probed by hybridization of γ-^{32}P-5′-end-labeled $(TTAGGG)_5$ oligonucleotide in 6 x SSC, 0.1 % SDS at 37 °C for 16-18 hr. The probed gel was washed twice for 5 min in 2 x SSC, 0.05 % SDS at room temperature, blotted on a piece of filter paper and air-dried. X-ray films (GE Healthcare, Little Chalfont, U.K.) were exposed to the probed gel for various amounts of time to ensure optimal resolution of DNA bands. The presence of t-circles in the original sample of ecDNA is inferred from the appearance of long, non-migrating single strands (RCA reaction products) of telomeric DNA on the probed gel. The gel bands resulting from

RCA were quantified using Bio-Rad Laboratories Quantity One gel analysis software (Bio-Rad Laboratories, Hercules, CA, U.S.A.).

2.5 Telomere Repeat Amplification Protocol (TRAP)

Cells were trypsinized, harvested in PBS and counted using a hemocytometer. Following centrifugation at 1,000 rpm for 5 min in a tabletop centrifuge (Beckman model TJ-6), the supernatant was aspirated and the cells were resuspended in CHAPS lysis buffer (10 mM Tris-HCl, pH 7.5; 1 mM $MgCl_2$; 1 mM EGTA; 0.1 mM benzamidine; 5 mM β-mercaptoethanol; 0.5 % w/v CHAPS; 10 % w/v glycerol) at a concentration of 1 x 10^5 cells/200 µL CHAPS buffer. The lysate was incubated on ice for 30 min, then centrifuged at 12,000 rpm for 30 min at 4 °C. The DNA-containing pellet was discarded and the protein-containing supernatant was fractionated into aliquots of 1 x 10^4 cell-equivalents and stored at -80 °C until use.

Serial ten-fold dilutions of the lysate supernatant (from 2,000 to 20 cell-equivalents) were prepared. Each TRAP reaction contained a total volume of 50 µL and was made up according to Table 1 in a 0.2 mL PCR tube. The samples were incubated for 20 min at room temperature for the telomerase extension reaction to proceed. The telomerase-extended products were then amplified using PCR in a thermocycler (MJ Research PTC-225; settings: 95 °C for 1 min, 50 °C for 45 s, 72 °C for 1 min; 30 cycles). The PCR products were loaded onto a 1 x Tris-borate-EDTA (TBE) polyacrylamide gel and separated by electrophoresis at 500 V for approximately 1 hr. The gel was stained with SYBR Green for 30 min at room

temperature and imaged using Quantity One gel analysis software (Bio-Rad Laboratories, Hercules, CA, U.S.A.).

Table 2.1 TRAP assay reaction mixture.

Reaction component	Volume (μL)
primer U2 (5′-ATCGCTTCTCGGCCTTTT-3′)	0.1
primer TSU2 (5′-AATCCGTCGAGCAGAGTTAAAA GGCCGAGAAGCGAT-3′)	0.1
primer ACX (5′-GCGCGGCTTACCCTTACCCTTACCCTAACC-3′)	0.1
primer TS (5′-AATCCGTCGAGCAGAGT -3′)	0.1
dNTP mix (25 mM each dNTP)	0.1
TRAP reaction buffer (10X)	5.0
Taq Polymerase (Boehringer Mannheim)	0.5
DEPC-treated H_2O	x = 50 - lysate volume - other components

2.6 Ectopic over-expression of telomerase in ALT cells

The hTERT-IRES-GFP and U3-hTR/PGK-YFP constructs used in this study were previously cloned into murine stem cell virus (MSCV)-based expression vectors and transduced into PG-13 murine virus packaging cells, in our laboratory. The vector-containing PG-13 cells were expanded at 37 °C and 5 % CO_2 in DMEM supplemented with 10 % FCS, 2 mM L-glutamine, 100 U/mL penicillin, and 0.1 mg/mL streptomycin. The packaged MSCV virus was released into the supernatant by incubating PG-13 cells in medium which is optimal for the VA-13 cells that were to be infected (MEM-α supplemented with 10 % FCS, 2 mM L-glutamine, 100 μM MEM non-essential amino acid solution, 100 U/mL penicillin, and 100 μg/mL streptomycin) at 32 °C, the optimal temperature for MSCV replication. After 48

hours of virus production, the supernatant was harvested, filtered through 0.45 μm pores, and stored in 5 mL aliquots at -80 °C until use.

The human ALT cell line, VA-13 was grown in 6-well plates and transduced with hTERT-IRES-GFP, U3-hTR/PGK-YFP, or both constructs by incubation with MSCV viral supernatant and media (1:1) overnight at 37 °C and 5 % CO_2. Since retroviral transduction occurs during cell division and VA-13 cells divide slowly, three rounds of transduction were performed to ensure that a sufficient number of VA-13 cells were transduced. The cells were washed in PBS and allowed to recover overnight by incubation in media between each round of infection, then expanded for several days. The cultures were sorted for expression of the transduced vectors by fluorescence-activated cell sorting (FACSVantage SE, Becton Dickinson, Franklin Lakes, NJ, U.S.A.). Three rounds of sorting and intervening expansion of the cell population were performed to obtain sufficiently pure cultures of transduced VA-13. Successful transduction was also confirmed by microscopic examination using the DeltaVision Core live cell imaging system (Applied Precision, Issaquah, WA, U.S.A.).

Chapter 3: Results

3.1 RCA amplifies telomeric sequence-containing circular plasmid DNA

RCA is an isothermal (30 °C) DNA replication reaction, catalyzed by the highly-processive Φ29 DNA polymerase, the enzyme responsible for replicating the 18 kb genome of the bacteriophage Φ29 [Watabe *et al.*, 1982]. Φ29 DNA polymerase has efficient strand displacement activity, which allows it to generate ssDNA products longer than 100 kb using small DNA circles as templates [Blanco and Salas, 1996; Lizardi *et al.*, 1998]. In the current study, the reaction was primed with a C-rich telomeric sequence 21mer oligonucleotide denoted "thio-C", because it contains two thiophosphate linkages between the three 3′ terminal nucleotides (see Chapter 2: Materials and Methods for primer sequence). Thiophosphate linkages prevent nucleolytic degradation of the primer by Φ29 DNA polymerase, which possesses 3′ to 5′ exonuclease activity acting preferentially on single-stranded DNA [Garmendia *et al.*, 1992]. An illustration of the RCA reaction is shown in Figure 3.1.

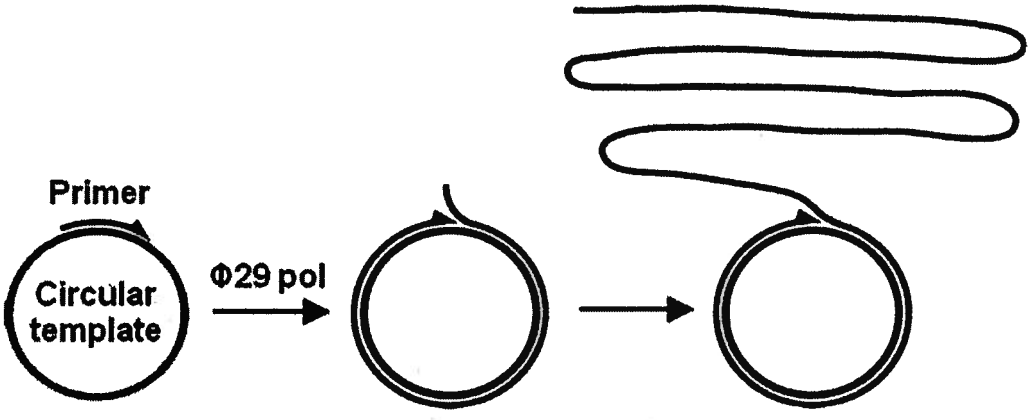

Figure 3.1 Rolling circle amplification. A simplified illustration of RCA catalyzed by Φ29 polymerase, resulting in the synthesis of a long ssDNA strand which consists of tandem replicates of the circle sequence.

In order to develop an RCA-based protocol to detect t-circles in human ALT cell lines, it was first necessary to optimize a protocol to amplify known amounts of purified telomere repeat-containing circular plasmid DNA *in vitro*. To this end, pBluescript II KS(+) plasmid vector containing an insert of 1.6 kb of telomeric repeat sequence (denoted "pTel 1.6") was used to template the RCA reaction.

Following thio-C-primed RCA of the pTel 1.6 template, a long ssDNA product was detected, which did not migrate from the wells during agarose gel electrophoresis (Figure 3.2; lanes 2-6). As a positive control, the reaction was primed with random sequence-containing, thiophosphate-modified hexamers, which are expected to amplify input DNA regardless of its sequence (Figure 3.2B; lane 2). As a negative control, the reaction was carried out in the absence of the Φ29 DNA polymerase (all other reaction components were included). No long ssDNA product was detected in the well when the polymerase was excluded (Figure 3.2; lane 1).

To determine the concentration of primer molecules that would yield the most ssDNA product following RCA, a titration of the thio-C primer was performed. The experiment revealed that the yield of the RCA reaction varies with respect to the primer concentration, when the amount of the template is held constant (Figure 3.2; lanes 3-6). The optimal concentration of thio-C primer to amplify approximately 150 ng of pTel template was shown to be between 1-3 μM (Figure 3.2; lanes 4 and 5).

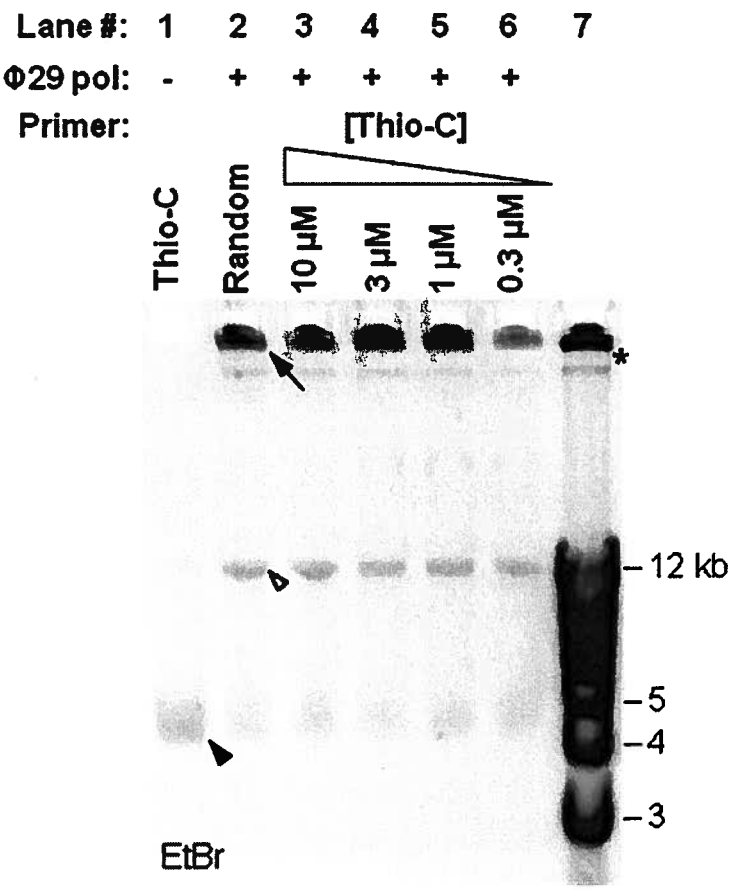

Figure 3.2 Amplification of plasmid DNA by RCA yields long, non-migrating ssDNA product. The circular plasmid pTel 1.6 was amplified using RCA primed with varying concentrations of the telomere-specific thio-C primer (lanes 3-6). The reaction yield of long ssDNA product (indicated by the arrow) was shown to be sensitive to the concentration of the thio-C primer in the reaction, with optimal yield seen at a concentration of 1-3 µM (lanes 4 and 5). Lane 1, negative control: the reaction mixture subjected to RCA conditions in the absence of Φ29 polymerase. Lane 2, positive control: RCA primed by random hexamer oligonucleotides. The black arrowhead indicates the pTel 1.6 plasmid; the white arrowhead likely indicates a concatemer of the highly recombinogenic pTel 1.6 plasmid DNA. The non-migrating DNA present in the 1 kb DNA size marker (lane 7, indicated by asterisk) results from association of smaller ladder fragments which contain sticky ends. This band can be resolved by denaturing gel electrophoresis (see Figure 3.10, which contains the same DNA ladder on a denaturing gel). EtBr, ethidium bromide.

To improve reaction efficiency and increase yield of the long ssDNA product, bacterial (*E. coli*) single-stranded DNA binding protein (SSB) was added to the reaction mixture. Previous work has shown that SSB improves the efficiency and accuracy of RCA, most likely by preventing the re-annealing of the ssDNA reaction product to the circular template, minimizing non-specific DNA products that may result from primer dimers, and potentially minimizing secondary structure formation [Inoue *et al.*, 2006]. An illustration of SSB binding during RCA is shown in Figure 3.3A.

In this study, 150 ng of pTel was used to template the reaction and 1 μM thio-C was used to prime the reaction. To determine the effects of SSB on RCA yield under these conditions, titres of SSB (concentration range 0 – 100 μg/mL) were added to each reaction (Figure 3.3B). The yield of the ssDNA reaction product was increased in the presence of SSB (Figure 3.3B; compare lanes 2 and 3). However, further increases of SSB concentration greater than 10 μg/mL did not appear to enhance the yield significantly (Figure 3.3B; lanes 3-6). This suggests that most of the ssDNA product is saturated with SSB binding at a concentration of 10 μg/mL and additional SSB molecules do not have available binding targets.

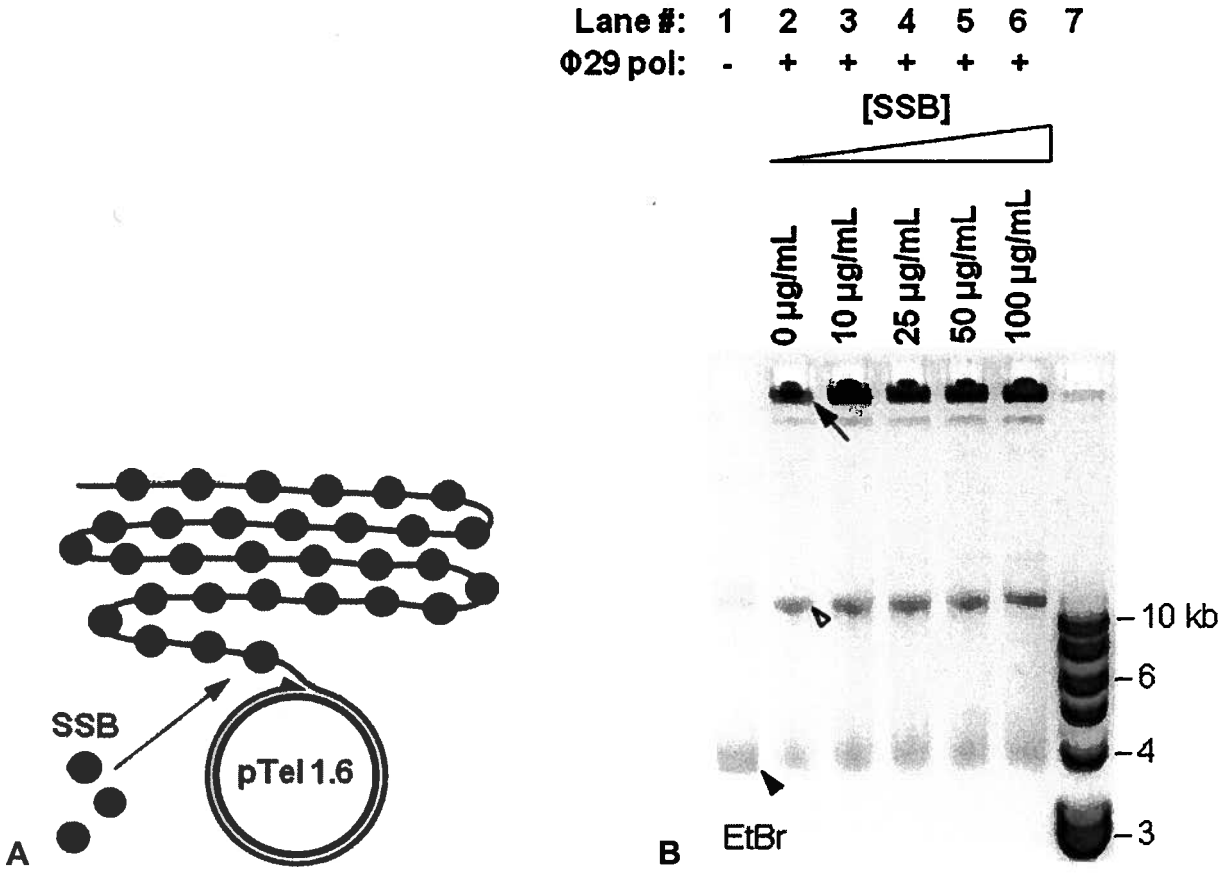

Figure 3.3 SSB improves the efficiency of RCA. (A) A schematic of *E. coli* SSB binding to the newly synthesized ssDNA as RCA proceeds. (B) The presence of SSB in during RCA increased the reaction product (lanes 2 and 3); however, increases of SSB concentration over 10 µg/mL did not further enhance RCA yield. Arrow indicates long ssDNA reaction product; the black arrowhead indicates the pTel 1.6 plasmid; the white arrowhead indicates concatenated plasmid DNA. EtBr, ethidium bromide.

3.2 RCA-based assay detects t-circles in the human ALT cell line GM847

To determine whether the RCA-based protocol will amplify t-circles in samples isolated from human cells, the protocol was applied to ecDNA extracts of the known, t-circle-containing, human ALT cell line, GM847. GM847 is an SV40-immortalized skin fibroblast [Henson *et al.*, 2002] which has long, heterogeneous telomeres and undetectable telomerase activity [Bryan *et al.*, 1995]. The presence of t-circles in GM847 cells was previously demonstrated using 2D PFGE and electron microscopy (EM) [Cesare and Griffith, 2004; Wang *et al.*, 2004]. In the current study, GM847 ecDNA was isolated using a modified Hirt extraction procedure [Hirt, 1967]. Hirt extraction consists of cell lysis using SDS, DNA precipitation in the presence of high NaCl concentration, and centrifugation to separate chromosomal DNA in the pellet from low molecular weight ecDNA in the supernatant (see Chapter 2: Materials and Methods for details). T-circles present in the GM847 ecDNA extract were subsequently taken through the thio-C-primed RCA procedure. The reaction product was separated by denaturing agarose gel electrophoresis, probed by in-gel hybridization of γ-^{32}P-5′-end-labeled $(TTAGGG)_5$ oligonucleotide, and visualized by exposure of X-ray films.

In order to establish whether conditions optimized to amplify pTel plasmid were consistent with those required for amplification of t-circles in GM847 ecDNA, titrations of thio-C primer and *E. coli* SSB protein were performed. T-circles present in the ecDNA extract of 2 x 10^5 GM847 cells served as templates for each reaction. Titration of thio-C primer molecules revealed that the highest levels of ssDNA product were obtained at a primer concentration of 0.1-1 μM (Figure 3.4A; lanes 4 and 5). Thio-C concentrations below 0.01 μM were

insufficient to yield any detectable product (Figure 3.4A; lanes 1 and 2). On the opposite end of the spectrum, concentrations above 10 μM seem to inhibit RCA extension by Φ29 DNA polymerase, presumably by saturating the t-circle templates with thio-C primer molecules (Figure 3.4A; lane 7). This data indicates that RCA is highly sensitive to the relative concentrations of primer and template molecules in the reaction.

Titration of SSB showed a positive correlation between increasing SSB concentration in the RCA reaction mix and the yield of ssDNA produced by the reaction (Figure 3.4B). In contrast with the results obtained from amplification of pTel 1.6 plasmids, increasing the SSB concentration above 10 µg/mL further increased the yield of ssDNA RCA product (compare Figures 3.3B and 3.4B). Several factors may be responsible for this discrepancy. First, the concentration of t-circles in ecDNA extracted from 2 x 10^5 GM847 cells may be significantly higher than the approximately 150 ng of pTel 1.6. An increased amount of template will yield a greater amount of ssDNA reaction product, providing more available binding sites for SSB. Second, larger circular templates would likewise yield more ssDNA product by providing more primer binding sites. If a significant proportion of t-circles in GM847 are larger than 1.6 kb (the length of telomeric DNA in a molecule of pTel 1.6), saturation of the product with SSB would occur at higher SSB concentrations. Finally, ecDNA extracts contain linear telomeric ecDNA molecules (much of which is G-rich ssDNA [Nabetani and Ishikawa, 2009]) and chromosomal telomeric DNA which may have sheared off the ends of chromosomes during the extraction procedure. Indeed, a significant amount of "contaminating" chromosomal DNA has been shown to remain in the supernatant (ecDNA) fraction following Hirt extraction [Nabetani and Ishikawa, 2009]. Any telomeric DNA

molecules, and especially G-rich ssDNA, will compete with t-circles for thio-C primer binding. Addition of SSB to the RCA reaction may sequester appreciable amounts of non-t-circle telomeric ssDNA, freeing up primer molecules for t-circle binding. However, at higher SSB concentrations, the yield of the reaction would be expected to plateau (as in the reaction with plasmid template, Figure 3.3B) and eventually decrease as a significant proportion of the primer molecules themselves are bound by SSB.

Importantly, the optimization of thio-C and SSB reaction conditions showed that t-circle amplification products can be detected using RCA in the ALT cell line GM847. These reaction conditions may potentially be applied to screen other ALT cell lines for t-circles (see Section 3.4).

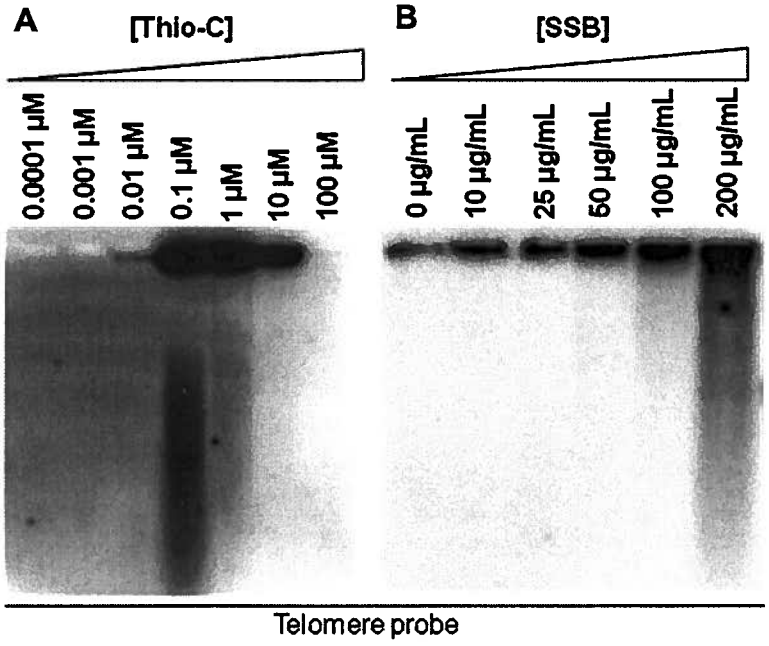

Figure 3.4 Determination of optimal thio-C and SSB concentrations to detect t-circles in GM847 ALT cells. (A) Titration of thio-C oligonucleotide primer reveals that optimal RCA yield was obtained using primer concentrations of 0.1-1 µM (lanes 4 and 5) when the t-circles in the ecDNA extract of 2 x 10^5 GM847 ALT cells were used as templates. (B) Titration of *E. coli* SSB shows that RCA-based t-circle detection in GM847 is enhanced by increasing the concentration of SSB.

3.3 Thio-C-primed RCA is a linear reaction which facilitates highly-sensitive detection of t-circles

RCA primed by a single, sequence-specific oligonucleotide normally proceeds with linear reaction kinetics and produces long ssDNA amplification products. However, RCA may likewise be primed by multiple oligonucleotides, such as in the reaction shown in Figure 3.2, lane 2; which was primed by random-sequence hexamers. This type of reaction is known as "hyperbranched" or "multiple displacement" RCA [Demidov, 2005] and has been used to generate high-fidelity templates for DNA sequencing from low-abundance circular vectors [Nelson *et al.*, 2002]. As a result of annealing and priming on already produced ssDNA, random primed-RCA proceeds with exponential geometric kinetics and yields hyperbranched dsDNA products [Demidov, 2005]. An illustration depicting linear and exponential RCA reactions is shown in Figure 3.5. Thio-C-primed RCA uses a single, sequence-specific oligonucleotide which can only anneal to one strand of telomeric DNA, producing an ssDNA replicate of the complimentary strand. Thus the reaction was expected to proceed with linear kinetics.

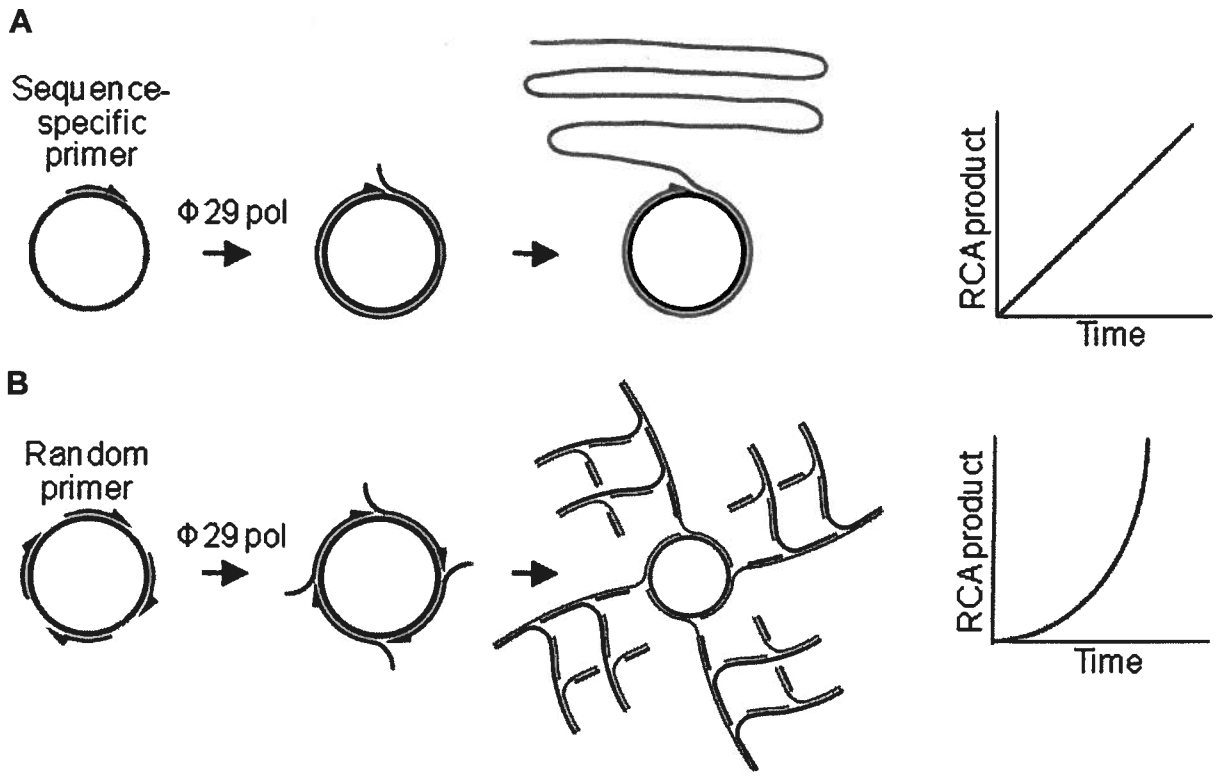

Figure 3.5 Linear *versus* exponential RCA reaction. (A) Extension of a single, sequence-specific primer by RCA yields increasing amounts of ssDNA in a linear fashion, on a plot of reaction time versus reaction yield. (B) Extension of multiple random sequence primers by RCA yields increasing amounts of dsDNA in an exponential manner.

To address the reaction dynamics of thio-C-primed RCA, a time-course experiment was conducted (Figure 3.6). T-circles present in ecDNA isolated from 2 x 10^5 GM847 ALT cells were used as template. Amplification time varied from 0 to 16 hours. Following denaturing agarose gel electrophoresis, probing with radioactively-labeled telomeric oligonucleotides, and exposure of an X-ray film, image analysis software was used to quantify the RCA reaction yield of long ssDNA (determined by the non-migrating band volume = band intensity x band area). Band volume quantification confirmed that thio-C-primed RCA of GM847 t-circles proceeds with linear reaction kinetics (Figure 3.8B).

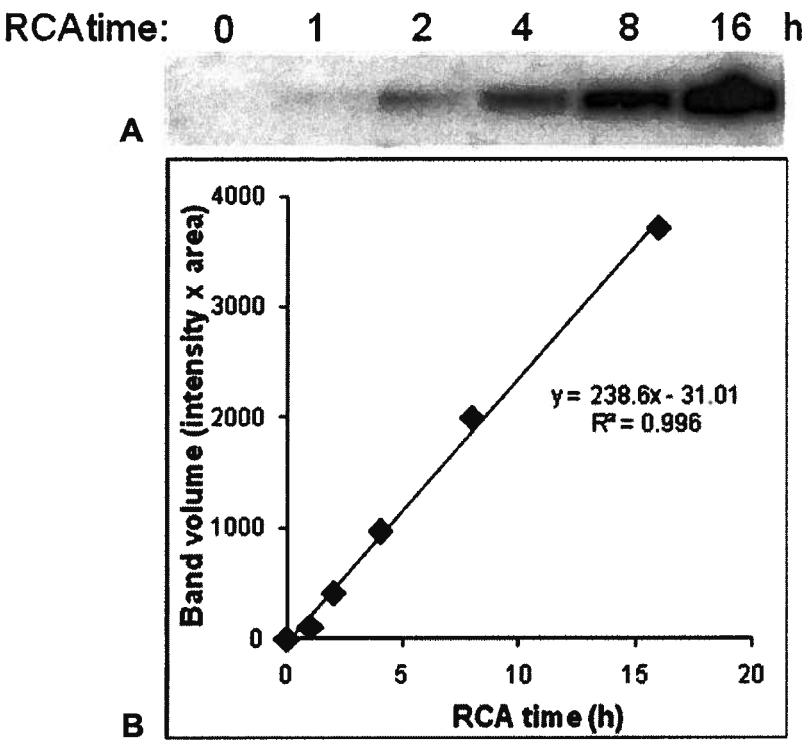

Figure 3.6 Time-course RCA. (A) ecDNA from 2 x 10^5 GM847 ALT cells was amplified by t-circle-specific RCA for the indicated amounts of time. T-circles were detectable following 1 hour of RCA. (B) Thio-C-primed RCA of t-circle templates proceeds with linear reaction kinetics.

To determine whether RCA-based detection of t-circles is more sensitive than the commonly-used 2D PFGE method which does not include any DNA amplification, titration of the ecDNA extract input was performed. T-circles present in the ecDNA extracts ranging from 5 x 10^3 to 4 x 10^5 GM847 cell-equivalents were used to template thio-C-primed RCA (Figure 3.9). Amplification products from t-circles were detectable in the ecDNA extract of as few as 5 x 10^3 cells. Thus t-circles were detected with a much higher sensitivity than what is possible using 2D PFGE, which commonly utilizes DNA extracted from at least 1.5 x 10^6 ALT cells [Cesare and Griffith, 2004; Wang *et al.*, 2004; Wang *et al.*, 2004].

RCA yield increased in a linear fashion relative to the input cell number until it reached a plateau at approximately 2 x 10^5 cell-equivalents (Figure 3.7B). This plateau likely represents the point at which no more primer molecules are available to bind the extra t-circles in the sample. If this is the case, addition of higher amounts of thio-C primer to the RCA would allow the reaction to proceed linearly with higher input ecDNA. Alternately, the amount of SSB and/or Φ29 DNA polymerase may likewise be limiting at higher t-circle template concentrations. Using the above-described reaction conditions, ecDNA extracts from 2 x 10^5 cell-equivalents were used as the template for all subsequent experiments.

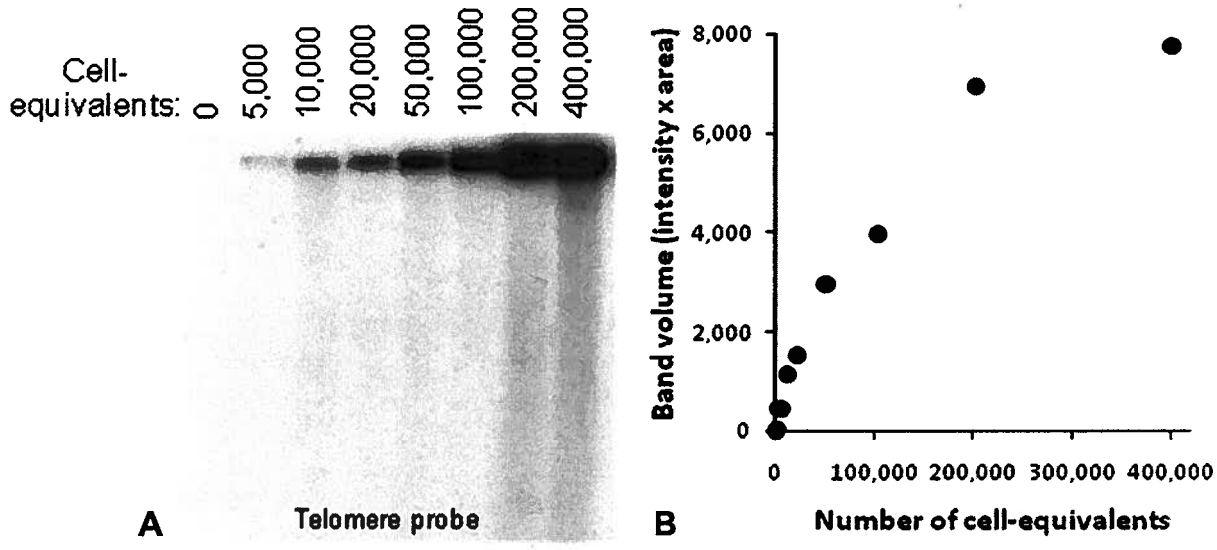

Figure 3.7 Titration of cell number in the RCA reaction. (A) ecDNA from the indicated number of GM847 ALT cells was extracted and subjected to t-circle-specific RCA. (B) A plot of the number of cell-equivalents per ecDNA extract used in the RCA reaction *versus* the reaction yield of long ssDNA as quantified by the non-migrating band volume.

3.4 RCA detects t-circles in human ALT cell lines but not in human telomerase-utilizing cell lines

To evaluate whether the RCA-based t-circle detection method that was optimized for GM847 ALT cells is applicable for screening purposes, a panel of cell lines was evaluated using this technique. The ecDNA extracts of established ALT-utilizing and telomerase-utilizing human immortalized cell lines were subjected to thio-C-primed RCA. The characteristics of these cell lines are summarized in Table 3.1.

Table 3.1 Cell lines used in the RCA-based screen for t-circles.

Cell line	Cell type	Transformation	TMM*
HeLa	Epithelial, cervix	Spontaneous	Telomerase
HCT116	Epithelial, colon	Spontaneous	Telomerase
GM847	Fibroblast, skin	SV40	ALT
SUSM-1	Fibroblast, liver	Chemical	ALT
VA-13	Fibroblast, lung	SV40	ALT

* TMM, telomere maintenance mechanism

For controls within this study, RCA was again used to amplify pTel 1.6 plasmid DNA. The negative control reaction was carried out in the absence of Φ29 DNA polymerase (Figure 3.8; lanes 2 and 4), whereas the positive control reaction was carried out in the presence of the enzyme (Figure 3.8; lanes 3 and 5). As expected, the control experiment revealed that RCA only proceeded in the presence of Φ29 DNA polymerase. However, probing of the gel with radioactively-labeled telomeric oligonucleotides revealed that telomeric DNA in the non-migraing ssDNA product was detected with extremely low efficiency (compare the relative amounts of pTel 1.6 plasmid and ssDNA RCA product as they appear on the ethidium bromide (EtBr)-stained gel and after probing, in lanes 3 and 5, respectively). The

low efficiency of probing for the long ssDNA product may potentially result from the presence of intervening plasmid vector sequences, or from an inability of the probe to hybridize to DNA which was essentially "clumped" within the well during overnight denaturing gel electrophoresis. This finding indicates that probing of the ssDNA RCA product may likewise be inefficient in amplified ecDNA extracts from cell lines.

Nevertheless, RCA reproducibly detected t-circles in the ALT cell lines GM847, SUSM-1, and VA-13, but did not detect any t-circles in the telomerase-utilizing cell lines HeLa and HCT116 (Figure 3.8; lanes 7-11). The observations are in agreement with previous studies where both types of cell lines were analyzed by 2D PFGE and EM [Cesare and Griffith, 2004; Wang *et al.*, 2004].

Interestingly, GM847 and SUSM-1 consistently showed a higher level of t-circles than VA-13 when the same number (2×10^5) of cell-equivalents was analyzed. This may be attributed to VA-13 having lower number of t-circles. On the other hand, the result may be an artifact of the amplification-based method. It is feasible that the RCA reaction conditions optimized for t-circle detection in GM847 are suboptimal in amplifying t-circles in VA-13 ecDNA extracts. For example, the RCA reaction may potentially proceed with a higher efficiency if a different number of cell-equivalents or thio-C primers were used.

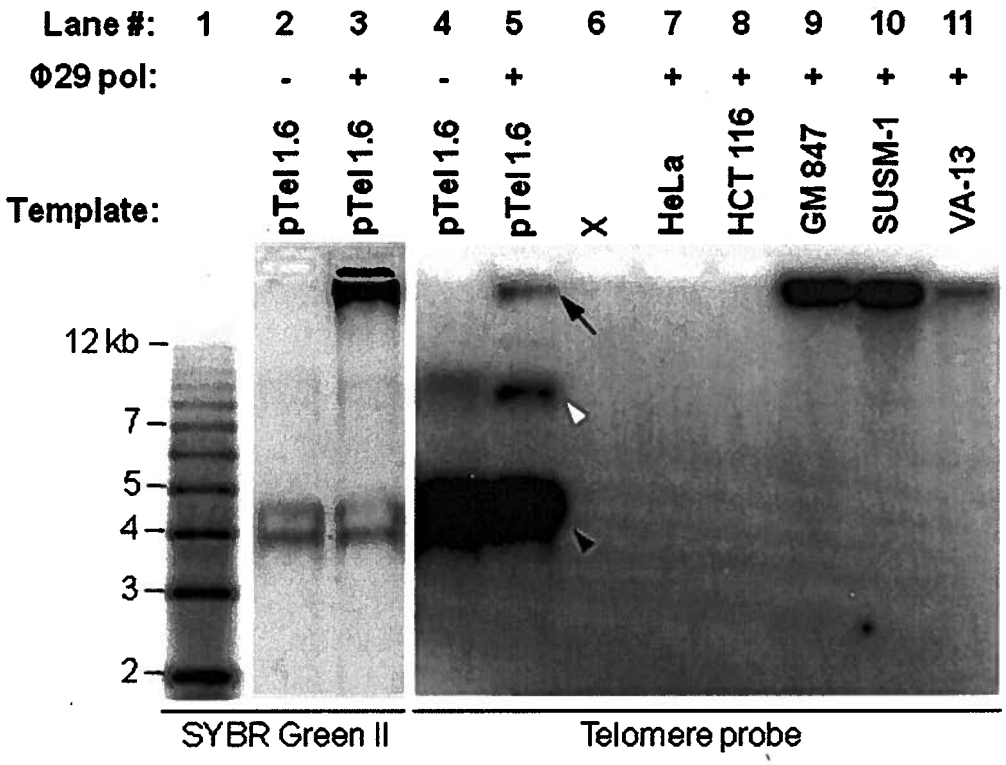

Figure 3.8 RCA-based screen detects t-circles in human ALT cell lines. pTel 1.6 was used as a control template to ensure the RCA reaction proceeded in the presence of Φ29 polymerase (lanes 2 and 4), but not in its absence (lanes 3 and 5). T-circles were detected in the ALT cell lines GM847, SUSM-1 and VA-13, but not in the telomerase-utilizing cell lines HeLa and HCT116. "X" (lane 6) indicates that no sample was loaded. Arrow indicates long ssDNA reaction product; the black arrowhead indicates the pTel 1.6 plasmid; the white arrowhead indicates concatenated plasmid DNA.

3.5 Telomerase reconstitution in ALT cells does not affect t-circle formation

Based on the existence of ALT-specific cellular phenotypes (e.g., telomeric recombination, APBs, MS32 instability, telomeric ecDNA) and the absence of t-circles in the telomerase-expressing cell lines evaluated above, we postulated that telomere maintenance by telomerase and ALT are mutually exclusive in a given cell line. This appears to be the case in yeast [Teng and Zakian, 1999], but studies of human ALT cell lines have produced conflicting observations [Cerone *et al.*, 2001; Ford *et al.*, 2001; Grobelny *et al.*, 2001; Perrem *et al.*, 2001; Wen, 1998] (see Chapter 4: Discussion). To directly assess whether reconstitution of telomerase activity affects t-circle generation in ALT cells, the telomerase components hTERT and hTR were ectopically overexpressed in VA-13 ALT cells. hTERT, the reverse transcriptase subunit of telomerase, catalyzes the addition of telomeric repeats to the 3′ end of the telomere using the hTR RNA subunit as template.

VA-13 cells were transduced by murine stem cell virus (MSCV)-derived expression vectors (previously cloned in our laboratory) using a retroviral infection protocol. Since VA-13 cells grow relatively slowly and are only transduced during cellular replication, three rounds of MSCV infection were performed to ensure sufficient transduction efficiency. The hTERT-containing construct (called MSCV-hTERT-IRES-GFP) expresses green fluorescent protein (GFP) from an internal ribosome entry site (IRES). The hTR-containing construct (called U3-hTR/PGK-YFP) expresses hTR from a U3 promoter and yellow fluorescent protein (YFP) from a separate, phosphoglycerin kinase (PGK) promoter. GFP and YFP were included in the vectors to facilitate tracking of transgene expression in the transduced cells. Simplified maps of these constructs are shown in Figure 3.9.

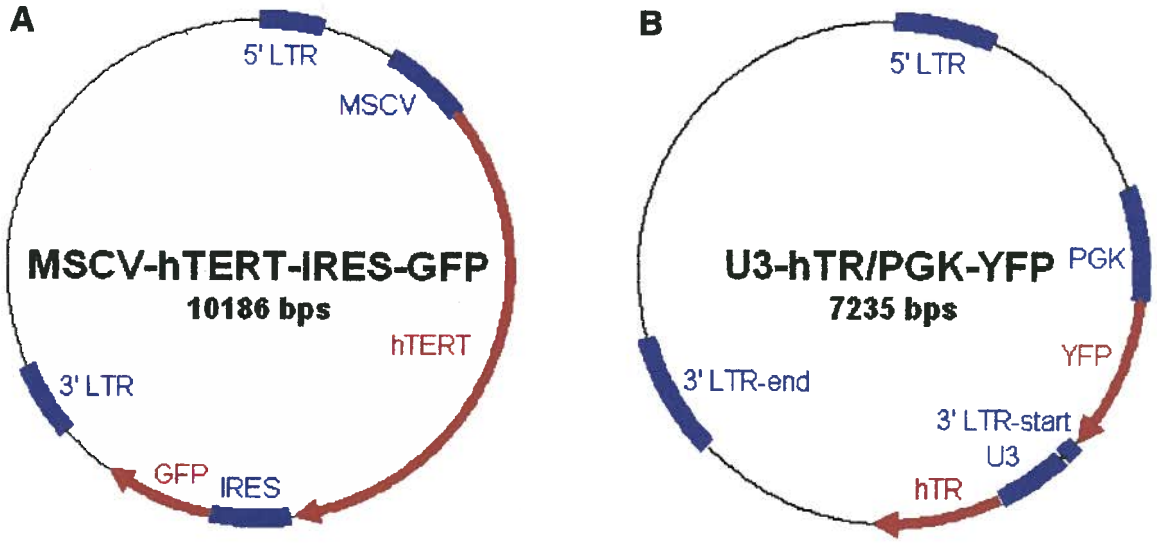

Figure 3.9 MSCV-based expression constructs containing telomerase subunits. (A) MSCV-hTERT-IRES-GFP. (B) U3-hTR/PGK-YFP. Displayed are the cloned genes, fluorescent proteins, promoter regions and the 5′ and 3′ long terminal repeat (LTR) regions, which are used to integrate retroviral DNA into host genomes.

The transduced cells were examined under a fluorescence microscope for expression of the fluorescent proteins. GFP (peak emission wavelength = 514 nm) and YFP (peak emission wavelength = 535 nm) cannot be distinguished using our fluorescence microscope, which detects both using the same filter. Thus fluorescence-activated cell sorting (FACS) was used to confirm their expression in the cells doubly-transduced with both constructs. To obtain cultures of sufficient purity, transduced cells were sorted three times by FACS for the expression of GFP, YFP, or both. The resulting purity values at the time of ecDNA isolation were approximately 63 % for the VA-13 cells over-expressing hTERT, 92 % for cells over-expressing hTR, and 62 % for cells over-expressing both hTERT and hTR. Representative microscope images and FACS purity plots are shown in Figure 3.10.

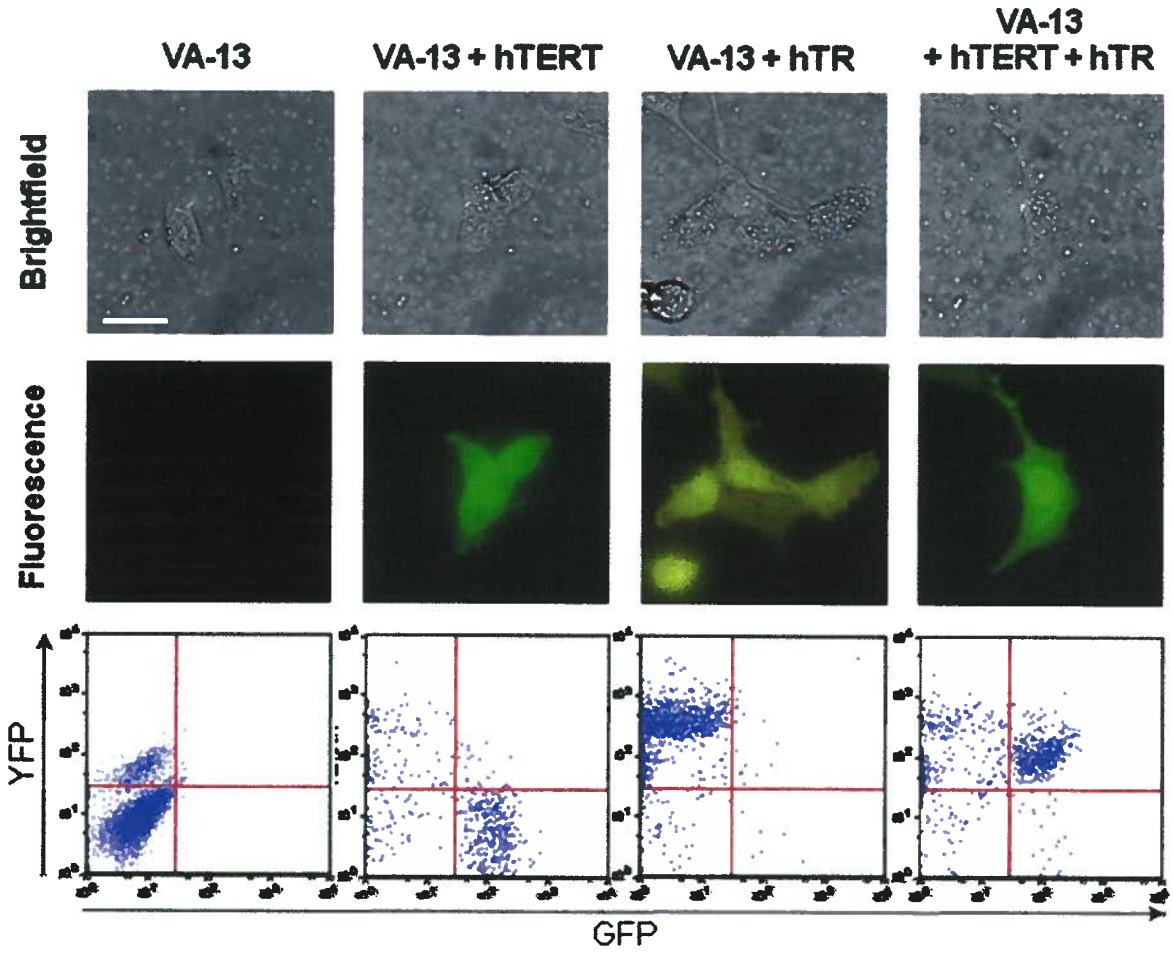

Figure 3.10 Expression of telomerase components in VA-13 ALT cells. Expression of the MSCV-based constructs MSCV-hTERT-IRES-GFP and U3-hTR/PGK-YFP in VA-13 ALT cells was confirmed by microscopy and FACS analysis. Representative images of cells under brightfield (top panels) and fluorescent (middle panels) illumination are shown. Note that the fluorescence images are pseudo-coloured, due to the fact that GFP and YFP emission cannot be discerned using our equipment. FACS analysis (purity plots shown in the bottom panels) confirmed that both constructs were expressed in the doubly-transduced VA-13 ALT cells. Even after three rounds of sorting, significant variation in the expression of the fluorescent proteins was observed. The size marker in the top left panel is 30 μm.

To determine whether expression of telomerase components lead to reconstitution of an active telomerase complex in doubly-transduced VA-13, a telomere repeat amplification protocol (TRAP) assay was performed (Figure 3.11). The TRAP assay relies on endogenous telomerase within protein extracts from a sample of cells to add 6 bp telomeric repeats to a set of specially designed oligonucleotides (see Chapter 2: Materials and Methods for the sequences). Addition of telomeric repeats is visualized as a "ladder" when amplified by PCR and separated by polyacrylamide gel electrophoresis. A 50 bp PCR product results from oligonucleotide annealing in the absence of addition of any telomeric repeats and serves as an internal control band (indicated by an arrow in Figure 3.11). In this experiment, the leukemic lymphoblast cell line K-562, which is known to express active telomerase, was used as a positive control (Figure 3.11, lanes 3-6). Untransduced VA-13 cells served as the negative control (Figure 3.11, lanes 7-10). 10-fold titrations of protein extracts of 2,000, 200 and 20 cell-equivalents of each cell type were included in the assay. Additional negative controls for all cell lines were provided by heat-inactivated (HI; 80 °C for 10 min) protein extracts from 2,000 cell-equivalents (Figure 3.11, lanes 6,10,14).

The TRAP assay revealed minor laddering in the untransduced VA-13 samples (indicated by a black arrowhead in Figure 3.11), although this cell line was previously shown to lack any detectable telomerase activity [Ford *et al.*, 2001; Wen, 1998]. Additional low molecular weight bands were also observed in the extracts of 2,000 and 200 cells in K-562 and VA-13 cell lines (indicated by a white arrowhead in Figure 3.11). These observations likely represent PCR artifacts due to oligonucleotide mispriming and indicate that further optimization of TRAP reaction conditions is necessary.

Nevertheless, these preliminary results showed that the doubly-transduced hTERT- and hTR-expressing VA-13 cells had significant telomerase activity (note the ladders in Figure 3.11, lanes 11-13). Telomerase activity in these cells was higher than in the telomerase-utilizing K-562 positive control cell line, presumably due to significant over-expression of the enzyme components. The reconstitution of telomerase activity in the ALT cell line VA-13 facilitates direct analysis of the effects of the telomerase enzyme on t-circle formation.

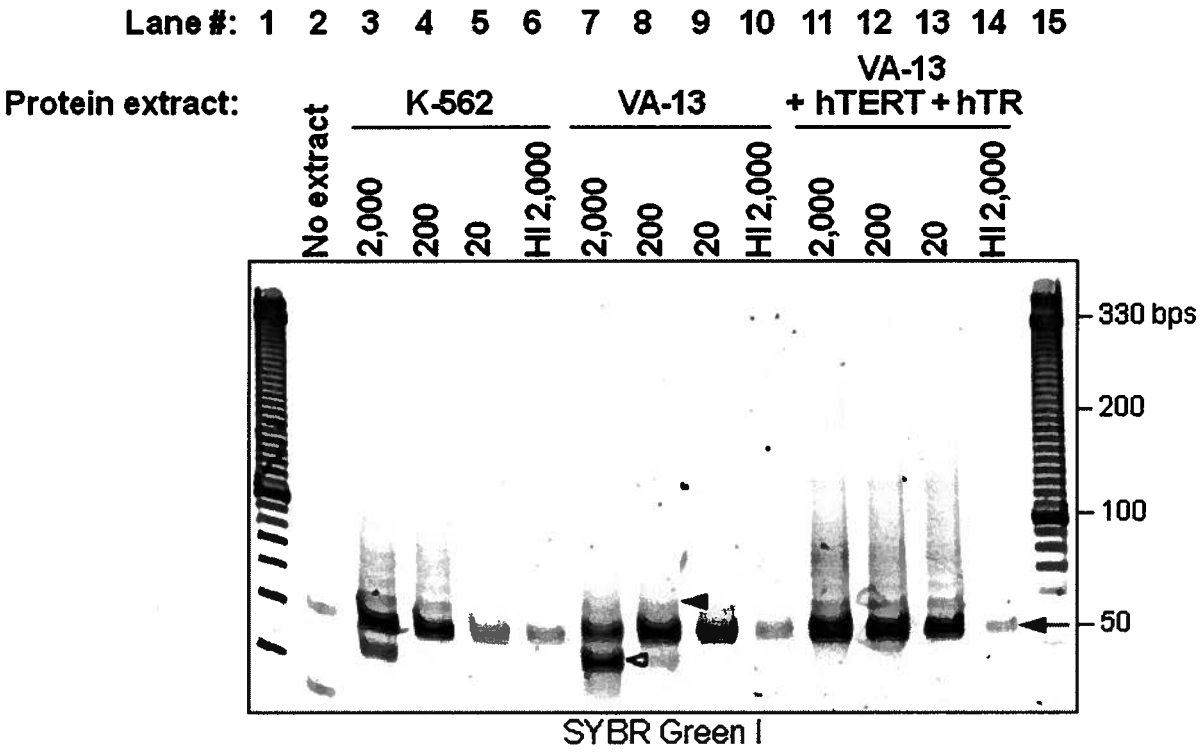

Figure 3.11 TRAP assay confirms reconstituted telomerase activity in VA-13 + hTERT + hTR cells. The telomerase-utilizing K-562 cell line showed telomerase activity in protein extracts from 2,000 and 200, but not 20 cell-equivalents. The ALT cell line VA-13 did not show any telomerase activity in any of the three extract titrations. The doubly-transduced VA-13 + hTERT + hTR cells displayed laddering in all three extract titrations, including the extract of only 20 cell-equivalents, indicating that the over-expressed telomerase components reconstituted an active telomerase enzyme complex. "No extract", negative control reaction which did not contain any protein extract but included all other TRAP components; HI, heat-inactivated protein extract from the indicated cell lines.

Based on the assumption that telomerase and ALT are mutually exclusive mechanisms for telomere maintenance, we hypothesized that t-circle formation would be inhibited in the presence of active telomerase. To address this possibility, the RCA-based t-circle assay was performed in VA-13, VA-13 over-expressing one of hTERT or hTR, and VA-13 over-expressing both hTERT and hTR, approximately 20 PDs after the final round of retroviral transduction. The 20 PD lag between transduction and t-circle detection was included to ensure that any t-circles already present in ALT cells at the time of telomerase reconstitution are diluted out via numerous cell divisions. Following RCA, no changes in t-circle levels were detected in the cells expressing active telomerase (VA-13 + hTERT + hTR) relative to control cells (Figure 3.12). It is possible that small changes in the amount of t-circles detected following telomerase reconstitution were obscured in this assay due to suboptimal purity of the doubly-transduced VA-13 cells (approximately 62 % at the time of ecDNA isolation). Nevertheless, these results indicate that telomerase activity does not completely inhibit t-circle formation in VA-13 ALT cells and suggests that telomeric recombination reactions can occur in the presence of telomerase.

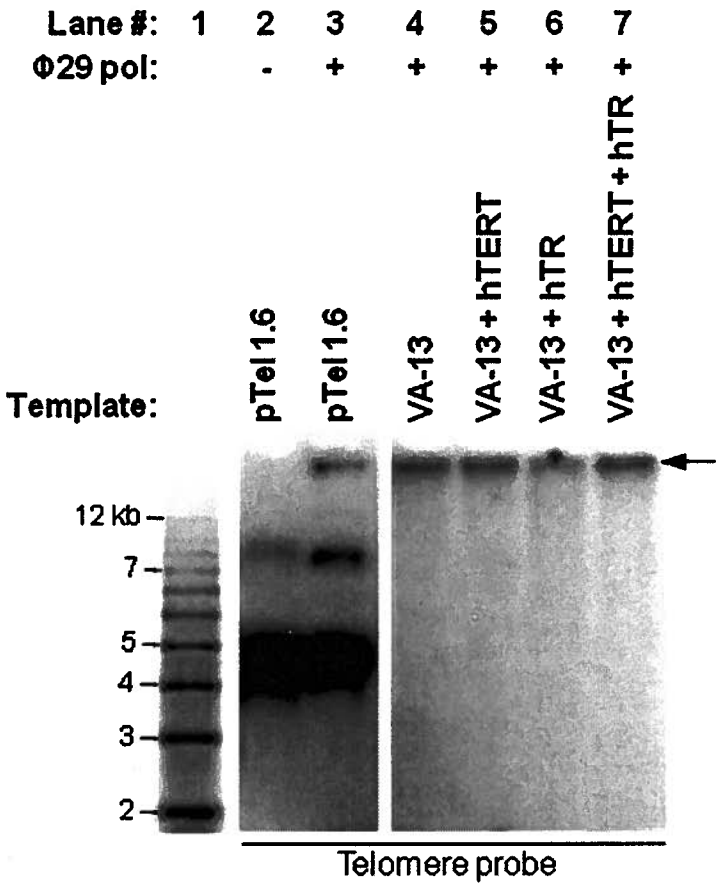

Figure 3.12 Telomerase reconstitution in VA-13 ALT cells does not affect t-circle formation. RCA-based detection of t-circles did not detect significant changes in t-circle levels in VA-13 ALT cells upon over-expression of active telomerase (compare lanes 4-7). Arrow indicates long ssDNA reaction product. (Note that the DNA size marker and the pTel-containing control lanes in this figure are the same as those shown in Figure 3.10. The two experiments were performed in parallel and RCA reaction products were run on the same denaturing agarose gel.)

Chapter 4: Discussion

4.1 RCA-based detection of t-circles is potentially more sensitive than the widely-used 2D PFGE method

In the current study, RCA was used to amplify t-circles in ecDNA extracts of human ALT cell lines. The amplification conditions were modified from the initially-published method [Zellinger *et al.*, 2007] by the use of ecDNA extracts instead of terminal restriction fragments (which contain chromosomal telomeres that are expected to sequester the thio-C primer) and by addition of *E. coli* SSB to the reaction mixture, which improved reaction efficiency. Using this protocol, t-circles were detected in ecDNA extracts of as few as 5 x 10^3 GM847 cell-equivalents under optimal conditions (Figure 3.9). It is possible that t-circles may be detected from even lower amounts of cells using the RCA-based method. To address this, further cell number titration experiments are necessary, which will likely require further titration of thio-C primer, titration of SSB protein, and longer exposure of X-ray films to visualize the minute non-migrating bands indicative of ssDNA amplification product.

Nevertheless, the ability to detect t-circles from as few as 5 x 10^3 ALT cells is significantly more sensitive than neutral-neutral 2D PFGE, which has been used for t-circle detection in the vast majority of publications to date. 2D PFGE requires that terminal restriction fragments (TRFs) from approximately 1.5-3.5 x 10^6 human diploid cells be loaded onto a single gel [Cesare and Griffith, 2004; Wang *et al.*, 2004; Wang *et al.*, 2004]. 2D PFGE is based on the electrophoretic separation of DNA molecules by size in the first dimension and by molecular structure/topology (e.g., linear vs. circular, "relaxed" vs. supercoiled) in the

second dimension. This method takes advantage of the fact that a linear molecule migrates through a gel matrix at a different rate than a non-linear molecule of equal mass [Bell and Byers, 1983; Oppenheim, 1981]. Thus t-circles migrate through the gel in the second dimension (separation by molecular structure or shape) at a slower rate relative to linear DNA restriction fragments [Wang *et al.*, 2004]. Increased sensitivity of t-circle detection was expected from the RCA-based method since it involves DNA amplification. However, in the absence of experiments to directly compare the RCA and 2D PFGE techniques in parallel, we cannot at this time make quantitative conclusions about the increased sensitivity provided by RCA. Titration experiments comparing input DNA required for t-circle detection by RCA and 2D PFGE in parallel are needed to address this question

RCA-based t-circle detection has other advantages relative to 2D PFGE. RCA amplifies t-circles of any size, whereas t-circles smaller than approximately 2 kb are difficult or impossible to resolve on 2D gels [Nabetani and Ishikawa, 2009]. RCA can amplify t-circles as small as 40 nucleotides (Karel Riha, personal communication). Also, the ability of RCA-based detection to run multiple samples in a single gel streamlines t-circle detection of a collection of different samples. In contrast, only a single sample can be loaded on a 2D gel, so screens involving numerous samples require several gels and additional controls for the variability of hybridization efficiency between different gels and exposure differences between different X-ray films.

The disadvantages of RCA relative to 2D PFGE include lack of information about the molecular weight and structure (i.e., single- or double-stranded, relaxed or supercoiled) of t-

circle molecules in the sample, and the variability introduced as a result of enzymatic amplification. RCA-based t-circle analysis is indirect; the DNA fragments that are detected on denaturing gels are long ssDNA amplicons of t-circle templates, but are not the t-circles themselves. As with any amplification-based methods of high sensitivity, there is an increased risk that contaminating factors may produce artifacts and false positives.

In contrast, 2D PFGE detects t-circles directly. Thus 2D PFGE provides data on the t-circle size and structure, with the exception of t-circles smaller than approximately 2 kb, which cannot be resolved on 2D gels [Nabetani and Ishikawa, 2009]. In addition, the enzymatic amplification and indirect detection that serve as great advantages in the sensitivity of the RCA-based method may conversely pose some challenges to t-circle quantification. RCA yield is very sensitive to the relative concentrations of primer molecules, t-circle templates, and SSB in the RCA reaction. For example, the lower reaction yield from amplifying VA-13 compared to GM847 and SUSM-1 (Figure 3.10) may indicate suboptimal primer concentration relative to the t-circle templates specifically present in VA-13 ecDNA extracts. Therefore, interpretations of RCA data must take into consideration that different reaction conditions may be necessary for optimal amplification of various samples.

4.1.1 Detection of telomeric circles in single cells

All established t-circle detection methods require populations of cells. As a result, they cannot provide some desirable data about the molecular biology of t-circles in ALT cells. For example, the fraction of cells in a given ALT cell population that contains t-circles and the number of t-circles per cell are not known. It is unclear whether there is a relationship between t-circle size and abundance, and the lengths of chromosomal telomeres within

individual cells. Likewise, it is unknown whether t-circles are dynamically formed and degraded (or integrated into chromosomal telomeres by recombination) within given clones, or stably maintained through mitotic divisions. The development of *in situ* t-circle detection methods may provide these insights into t-circle biology, which are unattainable by currently-available methods.

One of the most attractive features of RCA is that it may provide the basis of t-circle detection within individual cell nuclei. Fluorescent *in situ* hybridization (FISH) of telomeric repeat-oligonucleotides can identify telomeric ecDNA [Ford *et al.*, 2001; Hande *et al.*, 2001] but does not tell us whether these molecules are t-circles, linear telomeric DNA, or the recently-identified t-complex DNA [Nabetani and Ishikawa, 2009]. Amplification by *in situ* RCA could potentially provide this distinction, since only t-circles (and not linear or t-complex molecules) would be expected to template very long telomere repeat-containing ssDNA products.

Indeed, RCA has been utilized as a highly specific *in situ* signal amplification method for direct visualization of limited targets, such as point mutations in interphase nuclei [Zhong *et al.*, 2001] and single antibody molecules bound to antigens [Schweitzer *et al.*, 2000]. These experiments relied on the addition of exogenously-synthesized DNA circles to template RCA. The reactions were primed by DNA oligonucleotides consisting of two regions joined by a linker. One region was complementary to the circle templates and another region was specific for the point mutation [Zhong *et al.*, 2001] or covalently linked to an antibody [Schweitzer *et al.*, 2000].

We aimed to adapt our RCA protocol to detect t-circles directly in GM847 ALT cells, grown and fixed on glass slides. Preliminary experiments were unsuccessful, showing abundant non-specific binding of the fluorescent probe used to detect the ssDNA amplification product. Fluorescently-labeled RCA products indicative of t-circles were not observed (data not shown). Unlike previously-described *in situ* RCA methods [Schweitzer *et al.*, 2000; Zhong *et al.*, 2001], which used exogenously-synthesized DNA circles to template the reaction, our method relies on endogenous t-circles to template the RCA. It is possible that in our experiment, t-circles were fixed to the glass slides or cross-linked to other molecules in a way that prevents primer annealing and/or polymerase extension around the entire molecule. We anticipate that further development of an RCA-based *in situ* t-circle detection method will require the optimization of several key experimental conditions, including fixation strategies, DNA denaturation and primer annealing, and (fluorescent) detection of the RCA extension product. Despite these technical challenges, the development of such a method remains desirable and should be pursued.

4.2 The effects of telomerase activity on the ALT pathway

As discussed earlier, the effects of telomerase activity on telomere maintenance by ALT are not well understood. An important insight into the evolutionary origins of t-circles and ALT was gained by studies of yeast with linear mitochondrial DNA (mtDNA). The mitochondria of *Candida parapsilosis* contain abundant circular molecules derived from telomeric repeats, in addition to linear mtDNA genomes [Tomaska *et al.*, 2000]. In a study which compared the mtDNA architecture of various *C. parapsilosis* subspecies, the presence of t-circles correlated with the occurrence of linear mitochondrial genomes [Rycovska *et al.*, 2004]. The

authors proposed that recombination-based telomere lengthening involving ecDNA t-circles constitutes an archaic telomere maintenance mechanism which accompanied the evolution of linear genomes from their circular ancestors. Subsequently, this mechanism was replaced by the enzyme telomerase, which provides a more efficient way to synthesize telomeric arrays and thus ensure stability for the linear chromosomal form [Nosek *et al.*, 2006]. ALT-utilization by mammalian tumour cells may thus be thought of as a reversion to an ancestral telomere maintenance mechanism in an aberrant physiological setting.

Consistent with the notion that telomerase has evolutionarily outcompeted recombination-based pathways of telomere maintenance, recombination-mediated telomere elongation in *S. cerevisiae* telomerase-null survivors (see Section 1.2.1) is repressed by reconstitution of telomerase activity [Teng and Zakian, 1999]. On the other hand, reconstitution of telomerase in human ALT cells has yielded divergent observations in some studies [Cerone *et al.*, 2001; Ford *et al.*, 2001; Grobelny *et al.*, 2001; Perrem *et al.*, 2001; Wen, 1998]. In the current study, ectopic over-expression of telomerase in the ALT cell line VA-13 did not affect t-circle levels detected using the RCA-based method, suggesting that telomerase activity does not affect telomere maintenance by ALT. Continued t-circle formation in the presence of telomerase shows that recombination reactions at the telomeres (at least those responsible for generating t-circles) may occur in telomerase-expressing cells. However, in the absence of telomere length analysis, it remains unclear whether t-circles contribute to elongation of chromosomal telomeres following telomerase reconstitution. Conversely, upon reconstitution, telomerase may be targeted to telomeres in a dominant manner and prevent the use of t-circles as templates for lengthening (Figure 4.1). The findings also indicate that t-

circle formation is inhibited in human telomerase-utilizing cancer cells, such as HeLa and HCT116 (Figure 3.8), by means other than the enzyme itself. These cells may contain an unidentified inhibitory factor, or (more likely) possess a different telomere length, telomere topology, and/or telomeric chromatin relative to ALT cells.

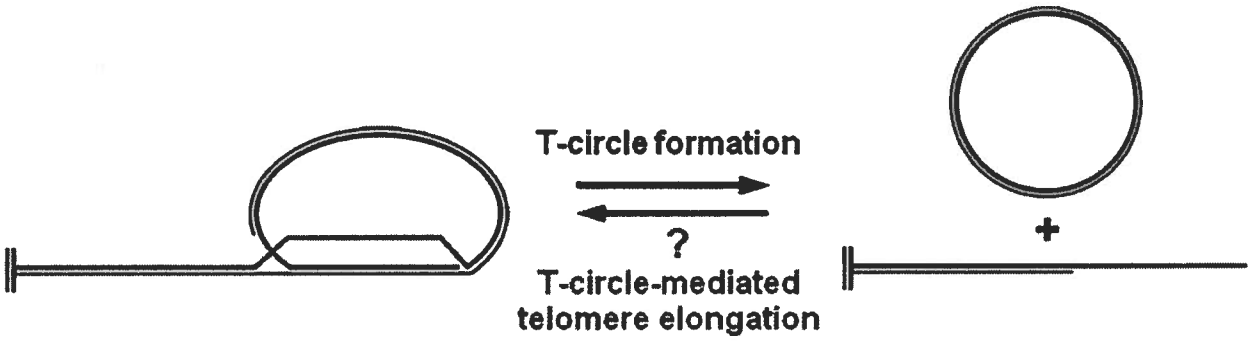

Figure 4.1 Telomere dynamics in VA-13 ALT cells over-expressing ectopic telomerase. Upon reconstitution of telomerase activity, t-circles continue to be formed in the VA-13 cell line. It remains unclear whether these t-circles contribute to telomere lengthening in the presence of telomerase, or whether they are inhibited from doing so by competition for the same molecular targets.

Several studies which evaluated other phenotypic characteristics of ALT concluded that telomerase and ALT can coexist and be concurrently active within a cell population [Cerone *et al.*, 2001; Grobelny *et al.*, 2001; Perrem *et al.*, 2001]. The long heterogeneous telomere length profile and the proportion of cells with APBs were shown to be unaffected by telomerase reconstitution [Cerone *et al.*, 2001; Grobelny *et al.*, 2001; Perrem *et al.*, 2001]. In one study, telomere length heterogeneity continued to be generated after more than 100 PDs with telomerase activity [Perrem *et al.*, 2001].

In contrast, there is limited evidence that utilization of ALT for telomere maintenance may be affected by telomerase over-expression in some cases. One group reported a loss of long heterogeneous telomeres and a reduction in the fraction of cells containing APBs in two of nine late passage GM847 ALT cell clones ectopically over-expressing telomerase [Ford *et al.*, 2001]. It is feasible that ALT-utilization may be lost as a stochastic event in some cells, which can continue to divide when exogenous telomerase is expressed. Alternately, ALT and telomerase may compete for access to the telomeres or other molecular targets and ALT may be repressed only in cases where a particularly high level of over-expressed telomerase subunits is present (Figure 4.1) [Henson *et al.*, 2002]. Further study of the molecular interactions between telomerase- and ALT-mediated telomere maintenance is needed to address these possibilities.

4.3 T-circles as by-products of overly long telomeres

Recently, several phenotypic characteristics that were considered exclusive to the ALT mechanism were observed in non-ALT immortalized human cell lines with ectopically enhanced telomerase activity [Pickett *et al.*, 2009]. The long-term effects of exogenous hTR over-expression in the telomerase-utilizing tumour cell lines HeLa and HT1080 resulted in increased telomerase activity, leading to long-term (~ 300 PDs) telomere lengthening. Telomere lengths also became more heterogeneous with increasing PDs, resembling the telomere length profile in ALT cells. However, important hallmarks of telomere maintenance by ALT were not detected. The hTR-over-expressing cells did not show an increased rate of T-SCEs and were unable to propagate a telomere-inserted tag to other telomeres, as was previously demonstrated in ALT cells [Dunham *et al.*, 2000; Londoño-Vallejo *et al.*, 2004].

However, other features of ALT, such as the presence of APBs, telomeric ecDNA, and t-circles were observed in these telomerase-utilizing cell lines. Thus these subnuclear structures likely represent by-products of overly long telomeres in ALT cells, rather than being --active mediators of telomere maintenance by ALT [Pickett *et al.*, 2009]. The findings suggest that in addition to telomere lengthening mechanisms, cells also have the means to shorten overly long telomeres by t-loop excision. An important implication of this work is that recombination reactions at the telomeres are triggered when telomere lengths become generally dysregulated; both when telomeres are too short (initiating ALT-mediated lengthening) [Morrish and Greider, 2009] and when they are too long [Pickett *et al.*, 2009].

Despite showing that t-circles are not restricted to the ALT pathway, these findings do not preclude the applicability of our RCA-based assay for t-circle detection in the context of categorizing human tumour samples based on their telomere maintenance mechanism. Human telomerase-utilizing cancer cells generally have short homogeneous telomere lengths, which would not be expected to generate t-circles at a high frequency. Conversely, the heterogeneity of telomere lengths in the majority of ALT-utilizing cancer cells means that a subset of telomeres reach a threshold length where t-loops would be excised to generate t-circles and other forms of ecDNA.

4.4 General conclusions

The major goal of this study was to develop an RCA-based assay for ALT status with the potential for screening tumour-derived samples from patients. RCA was optimized to amplify telomeric repeat-containing circular plasmid DNA as well as t-circles in ALT cell extracts. The technique allows indirect detection of t-circles from as few as 5×10^3 cells with the potential of further scaling down cell numbers. Additionally, multiple RCA-amplified samples can be loaded onto a single denaturing gel, allowing the screening of numerous samples in parallel. Therefore, this method of t-circle screening for ALT status has potential use in the clinic to screen for this tumour immortalization mechanism and thereby guide appropriate treatment.

An additional goal of this study was to determine if reactivation of the telomerase-based telomere lengthening mechanism would affect ALT-based telomere maintenance. Phenotypic markers of ALT, including t-circles evaluated in the current study, are generally absent in telomerase-utilizing cancer cells. We found that ectopic telomerase over-expression did not affect t-circle formation in the ALT cell line VA-13. This suggests that telomeric recombination reactions are not inhibited by telomerase, at least in this cell line. Further study is needed to determine the molecular interactions between telomerase and ALT pathways of telomere maintenance.

References

Allshire, R.C., Dempster, M. and Hastie, N.D. Human telomeres contain at least three types of G-rich repeat distributed non-randomly. *Nucleic Acids Res.* **17,** 4611-4627 (1989).

Amiard, S., Doudeau, M., Pinte, S., Poulet, A., Lenain, C., Faivre-Moskalenko, C., Angelov, D., Hug, N., Vindigni, A. and Bouvet, P. A topological mechanism for TRF2-enhanced strand invasion. *Nat. Struct. Mol. Biol.* **14,** 147-154 (2007).

Aubert, G. and Lansdorp, P.M. Telomeres and aging. *Physiol. Rev.* **88,** 557-579 (2008).

Bechter, O.E., Zou, Y., Shay, J.W. and Wright, W.E. Homologous recombination in human telomerase-positive and ALT cells occurs with the same frequency. *EMBO Rep.* **4,** 1138-1143 (2003).

Bell, L. and Byers, B. Separation of branched from linear DNA by two-dimensional gel electrophoresis. *Anal. Biochem.* **130,** 527-535 (1983).

Bernardi, R. and Pandolfi, P.P. Structure, dynamics and functions of promyelocytic leukaemia nuclear bodies. *Nat. Rev. Mol. Cell. Biol.* **8,** 1006-1016 (2007).

Bianchi, A., Smith, S., Chong, L., Elias, P. and de Lange, T. TRF1 is a dimer and bends telomeric DNA. *EMBO J.* **16,** 1785-1794 (1997).

Blanco, L. and Salas, M. Relating structure to function in phi 29 DNA polymerase. *J. Biol. Chem.* **271,** 8509-8512 (1996).

Bryan, T.M., Englezou, A., Gupta, J., Bacchetti, S. and Reddel, R.R. Telomere elongation in immortal human cells without detectable telomerase activity. *EMBO J.* **14,** 4240-4248 (1995).

Cerone, M.A., Londono-Vallejo, J.A. and Bacchetti, S. Telomere maintenance by telomerase and by recombination can coexist in human cells. *Hum. Mol. Genet.* **10,** 1945-1952 (2001).

Cesare, A.J. and Griffith, J.D. Telomeric DNA in ALT cells is characterized by free telomeric circles and heterogeneous t-loops. *Mol. Cell. Biol.* **24,** 9948-9957 (2004).

Costa, A., Daidone, M.G., Daprai, L., Villa, R., Cantu, S., Pilotti, S., Mariani, L., Gronchi, A., Henson, J.D., Reddel, R.R. and Zaffaroni, N. Telomere maintenance mechanisms in liposarcomas: association with histologic subtypes and disease progression. *Cancer Res.* **66,** 8918-8924 (2006).

d'Adda di Fagagna, F., Reaper, P.M., Clay-Farrace, L., Fiegler, H., Carr, P., von Zglinicki, T., Saretzki, G., Carter, N.P. and Jackson, S.P. A DNA damage checkpoint response in telomere-initiated senescence. *Nature* **426,** 194-197 (2003).

de Lange, T. Shelterin: the protein complex that shapes and safeguards human telomeres. *Genes Dev.* **19,** 2100-2110 (2005).

de Lange, T., Shiue, L., Myers, R.M., Cox, D.R., Naylor, S.L., Killery, A.M. and Varmus, H.E. Structure and variability of human chromosome ends. *Mol. Cell. Biol.* **10,** 518-527 (1990).

Demidov, V.V. Rolling-Circle Amplification (RCA). In: *Encyclopedia of Diagnostic Genomics and Proteomics.* Fuchs, J., and Podda, M., eds. New York, N.Y.: Marcel Dekker Incorporated. pp. 1175-1179 (2005).

Dunham, M.A., Neumann, A.A., Fasching, C.L. and Reddel, R.R. Telomere maintenance by recombination in human cells. *Nat. Genet.* **26,** 447-450 (2000).

Fasching, C.L., Neumann, A.A., Muntoni, A., Yeager, T.R. and Reddel, R.R. DNA damage induces alternative lengthening of telomeres (ALT) associated promyelocytic leukemia bodies that preferentially associate with linear telomeric DNA. *Cancer Res.* **67,** 7072-7077 (2007).

Ford, L.P., Zou, Y., Pongracz, K., Gryaznov, S.M., Shay, J.W. and Wright, W.E. Telomerase can inhibit the recombination-based pathway of telomere maintenance in human cells. *J. Biol. Chem.* **276,** 32198-32203 (2001).

Garmendia, C., Bernad, A., Esteban, J.A., Blanco, L. and Salas, M. The bacteriophage phi 29 DNA polymerase, a proofreading enzyme. *J. Biol. Chem.* **267,** 2594-2599 (1992).

Greider, C.W. and Blackburn, E.H. Identification of a specific telomere terminal transferase activity in Tetrahymena extracts. *Cell* **43,** 405-413 (1985).

Greider, C.W. and Blackburn, E.H. The telomere terminal transferase of Tetrahymena is a ribonucleoprotein enzyme with two kinds of primer specificity. *Cell* **51,** 887-898 (1987).

Griffith, J.D., Comeau, L., Rosenfield, S., Stansel, R.M., Bianchi, A., Moss, H. and de Lange, T. Mammalian telomeres end in a large duplex loop. *Cell* **97,** 503-514 (1999).

Grobelny, J.V., Godwin, A.K. and Broccoli, D. ALT-associated PML bodies are present in viable cells and are enriched in cells in the G (2)/M phase of the cell cycle. *J. Cell. Sci.* **113,** 4577-4585 (2000).

Grobelny, J.V., Kulp-McEliece, M. and Broccoli, D. Effects of reconstitution of telomerase activity on telomere maintenance by the alternative lengthening of telomeres (ALT) pathway. *Hum. Mol. Genet.* **10,** 1953-1961 (2001).

Hahn, W.C., Stewart, S.A., Brooks, M.W., York, S.G., Eaton, E., Kurachi, A., Beijersbergen, R.L., Knoll, J.H., Meyerson, M. and Weinberg, R.A. Inhibition of telomerase limits the growth of human cancer cells. *Nat. Med.* **5,** 1164-1170 (1999).

Hakin-Smith, V., Jellinek, D.A., Levy, D., Carroll, T., Teo, M., Timperley, W.R., McKay, M.J., Reddel, R.R. and Royds, J.A. Alternative lengthening of telomeres and survival in patients with glioblastoma multiforme. *Lancet* **361,** 836-838 (2003).

Hande, M.P., Balajee, A.S., Tchirkov, A., Wynshaw-Boris, A. and Lansdorp, P.M. Extra-chromosomal telomeric DNA in cells from Atm(-/-) mice and patients with ataxia-telangiectasia. *Hum. Mol. Genet.* **10,** 519-528 (2001).

Hande, M.P., Samper, E., Lansdorp, P. and Blasco, M.A. Telomere length dynamics and chromosomal instability in cells derived from telomerase null mice. *J. Cell Biol.* **144,** 589-601 (1999).

Henderson, E., Hardin, C.C., Walk, S.K., Tinoco, I.,Jr and Blackburn, E.H. Telomeric DNA oligonucleotides form novel intramolecular structures containing guanine-guanine base pairs. *Cell* **51,** 899-908 (1987).

Henderson, E.R. and Blackburn, E.H. An overhanging 3'terminus is a conserved feature of telomeres. *Mol. Cell. Biol.* **9,** 345-348 (1989).

Henson, J.D., Hannay, J.A., McCarthy, S.W., Royds, J.A., Yeager, T.R., Robinson, R.A., Wharton, S.B., Jellinek, D.A., Arbuckle, S.M., Yoo, J., Robinson, B.G., Learoyd, D.L., Stalley, P.D., Bonar, S.F., Yu, D., Pollock, R.E. and Reddel, R.R. A robust assay for alternative lengthening of telomeres in tumors shows the significance of alternative lengthening of telomeres in sarcomas and astrocytomas. *Clin. Cancer Res.* **11,** 217-225 (2005).

Henson, J.D., Neumann, A.A., Yeager, T.R. and Reddel, R.R. Alternative lengthening of telomeres in mammalian cells. *Oncogene* **21,** 598-610 (2002).

Hirt, B. Selective extraction of polyoma DNA from infected mouse cell cultures. *J. Mol. Biol.* **26,** 365-369 (1967).

Inoue, J., Shigemori, Y. and Mikawa, T. Improvements of rolling circle amplification (RCA) efficiency and accuracy using Thermus thermophilus SSB mutant protein. *Nucleic Acids Res.* **34,** e69 (2006).

Jeyapalan, J.N., Varley, H., Foxon, J.L., Pollock, R.E., Jeffreys, A.J., Henson, J.D., Reddel, R.R. and Royle, N.J. Activation of the ALT pathway for telomere maintenance can affect other sequences in the human genome. *Hum. Mol. Genet.* **14,** 1785-1794 (2005).

Jeyapalan, J.N., Mendez-Bermudez, A., Zaffaroni, N., Dubrova, Y.E. and Royle, N.J. Evidence for alternative lengthening of telomeres in liposarcomas in the absence of ALT-associated PML bodies. *Int. J. Cancer* **122,** 2414-2421 (2008).

Johnson, F.B., Marciniak, R.A., McVey, M., Stewart, S.A., Hahn, W.C. and Guarente, L. The Saccharomyces cerevisiae WRN homolog Sgs1p participates in telomere maintenance in cells lacking telomerase. *EMBO J.* **20,** 905-913 (2001).

Johnson, J.E., Varkonyi, R.J., Schwalm, J., Cragle, R., Klein-Szanto, A., Patchefsky, A., Cukierman, E., von Mehren, M. and Broccoli, D. Multiple mechanisms of telomere maintenance exist in liposarcomas. *Clin. Cancer Res.* **11,** 5347-5355 (2005).

Kilian, A., Bowtell, D.D.L., Abud, H.E., Hime, G.R., Venter, D.J., Keese, P.K., Duncan, E.L., Reddel, R.R. and Jefferson, R.A. Isolation of a candidate human telomerase catalytic subunit gene, which reveals complex splicing patterns in different cell types. *Hum. Mol. Genet.* **6,** 2011-2019 (1997).

Kim, N.W., Piatyszek, M.A., Prowse, K.R., Harley, C.B., West, M.D., Ho, P.L., Coviello, G.M., Wright, W.E., Weinrich, S.L. and Shay, J.W. Specific association of human telomerase activity with immortal cells and cancer. *Science* **266,** 2011-2015 (1994).

Lansdorp, P.M. Major cutbacks at chromosome ends. *Trends Biochem. Sci.* **30,** 388-395 (2005).

Lendvay, T.S., Morris, D.K., Sah, J., Balasubramanian, B. and Lundblad, V. Senescence mutants of Saccharomyces cerevisiae with a defect in telomere replication identify three additional EST genes. *Genetics* **144,** 1399-1412 (1996).

Liu, Y., Masson, J.Y., Shah, R., O'Regan, P. and West, S.C. RAD51C is required for Holliday junction processing in mammalian cells. *Science* **303,** 243-246 (2004).

Lizardi, P.M., Huang, X., Zhu, Z., Bray-Ward, P., Thomas, D.C. and Ward, D.C. Mutation detection and single-molecule counting using isothermal rolling-circle amplification. *Nat. Genet.* **19,** 225-232 (1998).

Londoño-Vallejo, J.A., Der-Sarkissian, H., Cazes, L., Bacchetti, S. and Reddel, R.R. Alternative lengthening of telomeres is characterized by high rates of telomeric exchange. *Cancer Res.* **64,** 2324-2327 (2004).

Lundblad, V. and Blackburn, E.H. An alternative pathway for yeast telomere maintenance rescues est1⁻ senescence. *Cell* **73,** 347-360 (1993).

Lundblad, V. and Szostak, J.W. A mutant with a defect in telomere elongation leads to senescence in yeast. *Cell* **57,** 633-643 (1989).

Lustig, A.J. Clues to catastrophic telomere loss in mammals from yeast telomere rapid deletion. *Nat. Rev. Genet.* **4,** 916-923 (2003).

Makarov, V.L., Hirose, Y. and Langmore, J.P. Long G tails at both ends of human chromosomes suggest a C strand degradation mechanism for telomere shortening. *Cell* **88,** 657-666 (1997).

Martens, U.M., Chavez, E.A., Poon, S.S.S., Schmoor, C. and Lansdorp, P.M. Accumulation of short telomeres in human fibroblasts prior to replicative senescence. *Exp. Cell Res.* **256,** 291-299 (2000).

Mattern, K.A., Swiggers, S.J.J., Nigg, A.L., Lowenberg, B., Houtsmuller, A.B. and Zijlmans, J.M. Dynamics of protein binding to telomeres in living cells: implications for telomere structure and function. *Mol. Cell. Biol.* **24,** 5587-5594 (2004).

McClintock, B. The Stability of Broken Ends of Chromosomes in Zea Mays. *Genetics* **26,** 234-282 (1941).

McEachern, M.J. and Blackburn, E.H. Cap-prevented recombination between terminal telomeric repeat arrays (telomere CPR) maintains telomeres in Kluyveromyces lactis lacking telomerase. *Genes Dev.* **10,** 1822-1834 (1996).

Morrish, T.A. and Greider, C.W. Short telomeres initiate telomere recombination in primary and tumor cells. *PLoS Genet.* **5,** e1000357 (2009).

Moyzis, R.K., Buckingham, J.M., Cram, L.S., Dani, M., Deaven, L.L., Jones, M.D., Meyne, J., Ratliff, R.L. and Wu, J.R. A highly conserved repetitive DNA sequence, (TTAGGG)n, present at the telomeres of human chromosomes. *Proc. Natl. Acad. Sci. U. S. A.* **85,** 6622-6626 (1988).

Müller, H.J. The re-making of chromosomes. *Collecting Net* **13,** 181-198 (1938).

Muntoni, A., Neumann, A.A., Hills, M. and Reddel, R.R. Telomere elongation involves intra-molecular DNA replication in cells utilizing alternative lengthening of telomeres. *Hum. Mol. Genet.* **18,** 1017-1027 (2009).

Muntoni, A. and Reddel, R.R. The first molecular details of ALT in human tumor cells. *Hum. Mol. Genet.* **14,** R191-R196 (2005).

Murnane, J.P., Sabatier, L., Marder, B.A. and Morgan, W.F. Telomere dynamics in an immortal human cell line. *EMBO J.* **13,** 4953-4962 (1994).

Nabetani, A. and Ishikawa, F. Unusual telomeric DNAs in human telomerase-negative immortalized cells. *Mol. Cell. Biol.* **29,** 703-713 (2009).

Natarajan, S. and McEachern, M.J. Recombinational telomere elongation promoted by DNA circles. *Mol. Cell. Biol.* **22,** 4512-4521 (2002).

Nelson, J.R., Cai, Y.C., Giesler, T.L., Farchaus, J.W., Sundaram, S.T., Ortiz-Rivera, M., Hosta, L.P., Hewitt, P.L., Mamone, J.A. and Palaniappan, C. TempliPhi, phi29 DNA polymerase based rolling circle amplification of templates for DNA sequencing. *Biotechniques* **32,** S44-S47 (2002).

Nosek, J., Kosa, P. and Tomaska, L. On the origin of telomeres: a glimpse at the pre-telomerase world. *Bioessays* **28,** 182-190 (2006).

Ogino, H., Nakabayashi, K., Suzuki, M., Takahashi, E., Fujii, M., Suzuki, T. and Ayusawa, D. Release of telomeric DNA from chromosomes in immortal human cells lacking telomerase activity. *Biochem. Biophys. Res. Commun.* **248,** 223-227 (1998).

Olovnikov, A.M. A theory of marginotomy. The incomplete copying of template margin in enzymic synthesis of polynucleotides and biological significance of the phenomenon. *J. Theor. Biol.* **41,** 181-190 (1973).

Oppenheim, A. Separation of closed circular DNA from linear DNA by electrophoresis in two dimensions in agarose gels. *Nucleic Acids Res.* **9,** 6805 (1981).

Park, K.H., Rha, S.Y., Kim, C.H., Kim, T.S., Yoo, N.C., Kim, J.H., Roh, J.K., Noh, S.H., Min, J.S., Lee, K.S., Kim, B.S. and Chung, H.C. Telomerase activity and telomere lengths in various cell lines: changes of telomerase activity can be another method for chemosensitivity evaluation. *Int. J. Oncol.* **13,** 489-495 (1998).

Perrem, K., Colgin, L.M., Neumann, A.A., Yeager, T.R. and Reddel, R.R. Coexistence of alternative lengthening of telomeres and telomerase in hTERT-transfected GM847 cells. *Mol. Cell. Biol.* **21,** 3862-3875 (2001).

Pickett, H.A., Cesare, A.J., Johnston, R.L., Neumann, A.A. and Reddel, R.R. Control of telomere length by a trimming mechanism that involves generation of t-circles. *EMBO J.* **28,** 799-809 (2009).

Poulet, A., Buisson, R., Faivre-Moskalenko, C., Koelblen, M., Amiard, S., Montel, F., Cuesta-Lopez, S., Bornet, O., Guerlesquin, F. and Godet, T. TRF2 promotes, remodels and protects telomeric Holliday junctions. *EMBO J.* **28,** 641-651 (2009).

Royle, N.J., Foxon, J., Jeyapalan, J.N., Mendez-Bermudez, A., Novo, C.L., Williams, J. and Cotton, V.E. Telomere length maintenance – an ALTernative mechanism. *Cytogenet. Genome Res.* **122,** 281-291 (2008).

Rycovska, A., Valach, M., Tomaska, L., Bolotin-Fukuhara, M. and Nosek, J. Linear versus circular mitochondrial genomes: intraspecies variability of mitochondrial genome architecture in Candida parapsilosis. *Microbiology* **150,** 1571-1580 (2004).

Schweitzer, B., Wiltshire, S., Lambert, J., O'Malley, S., Kukanskis, K., Zhu, Z., Kingsmore, S.F., Lizardi, P.M. and Ward, D.C. Immunoassays with rolling circle DNA amplification: a versatile platform for ultrasensitive antigen detection. *Proc. Natl. Acad. Sci. U. S. A.* **97,** 10113-10119 (2000).

Stewart, S.A. Telomere maintenance and tumorigenesis: an "ALT"ernative road. *Curr. Mol. Med.* **5,** 253-257 (2005).

Stuurman, N., de Graaf, A., Floore, A., Josso, A., Humbel, B., de Jong, L. and van Driel, R. A monoclonal antibody recognizing nuclear matrix-associated nuclear bodies. *J. Cell. Sci.* **101,** 773-784 (1992).

Sudbery, P. Highly repetitive DNA. In: *Human molecular genetics.* 2nd ed. Harlow, U.K.: Pearson Education Limited. pp. 39-41 (2002).

Teng, S.C. and Zakian, V.A. Telomere-telomere recombination is an efficient bypass pathway for telomere maintenance in Saccharomyces cerevisiae. *Mol. Cell. Biol.* **19,** 8083-8093 (1999).

Tokutake, Y., Matsumoto, T., Watanabe, T., Maeda, S., Tahara, H., Sakamoto, S., Niida, H., Sugimoto, M., Ide, T. and Furuichi, Y. Extra-chromosomal telomere repeat DNA in telomerase-negative immortalized cell lines. *Biochem. Biophys. Res. Commun.* **247,** 765-772 (1998).

Tomaska, L., Nosek, J., Makhov, A.M., Pastorakova, A. and Griffith, J.D. Extragenomic double-stranded DNA circles in yeast with linear mitochondrial genomes: potential involvement in telomere maintenance. *Nucleic Acids Res.* **28,** 4479-4487 (2000).

Tomaska, L., McEachern, M.J. and Nosek, J. Alternatives to telomerase: keeping linear chromosomes via telomeric circles. *FEBS Lett.* **567,** 142-146 (2004).

Varley, H., Pickett, H.A., Foxon, J.L., Reddel, R.R. and Royle, N.J. Molecular characterization of inter-telomere and intra-telomere mutations in human ALT cells. *Nat. Genet.* **30,** 301-305 (2002).

Wang, R.C., Smogorzewska, A. and de Lange, T. Homologous recombination generates T-loop-sized deletions at human telomeres. *Cell* **119,** 355-368 (2004).

Watabe, K., Shih, M.F., Sugino, A. and Ito, J. In vitro Replication of Bacteriophage 29 DNA. *Proc. Natl. Acad. Sci. U. S. A.* **79,** 5245-5248 (1982).

Watson, J.D. Origin of concatemeric T7 DNA. *Nat. New Biol.* **239,** 197-201 (1972).

Wen, J. Reconstitution of wild-type or mutant telomerase activity in telomerase-negative immortal human cells. *Hum. Mol. Genet.* **7,** 1137-1141 (1998).

Wu, G., Jiang, X., Lee, W.H. and Chen, P.L. Assembly of functional ALT-associated promyelocytic leukemia bodies requires Nijmegen Breakage Syndrome 1. *Cancer Res.* **63,** 2589-2595 (2003).

Wu, G., Lee, W.H. and Chen, P.L. NBS1 and TRF1 Colocalize at Promyelocytic Leukemia Bodies during Late S/G2 Phases in Immortalized Telomerase-negative Cells. Implication of NBS1 in alternative lengthening of telomeres. *J. Biol. Chem.* **275,** 30618-30622 (2000).

Yankiwski, V., Marciniak, R.A., Guarente, L. and Neff, N.F. Nuclear structure in normal and Bloom syndrome cells. *Proc. Natl. Acad. Sci. U. S. A.* **97,** 5214-5219 (2000).

Yeager, T.R., Neumann, A.A., Englezou, A., Huschtscha, L.I., Noble, J.R. and Reddel, R.R. Telomerase-negative immortalized human cells contain a novel type of promyelocytic leukemia (PML) body. *Cancer Res.* **59,** 4175-4179 (1999).

Zakian, V.A. Structure and function of telomeres. *Annu. Rev. Genet.* **23,** 579-604 (1989).

Zellinger, B., Akimcheva, S., Puizina, J., Schirato, M. and Riha, K. Ku suppresses formation of telomeric circles and alternative telomere lengthening in Arabidopsis. *Mol. Cell* **27,** 163-169 (2007).

Zhong, X., Lizardi, P.M., Huang, X., Bray-Ward, P.L. and Ward, D.C. Visualization of oligonucleotide probes and point mutations in interphase nuclei and DNA fibers using rolling circle DNA amplification. *Proc. Natl. Acad. Sci. U. S. A.* **98,** 3940-3945 (2001).